Open Access Articles

Dynamics of wind-driven estuarine-shelf exchange in the Narragansett Bay estuary

The Faculty of Oregon State University has made this article openly available.
Please share how this access benefits you. Your story matters.

Citation	Pfeiffer-Herbert, A. S., Kincaid, C. R., Bergondo, D. L., & Pockalny, R. A. (2015). Dynamics of wind-driven estuarine-shelf exchange in the Narragansett Bay estuary. Continental Shelf Research, 105, 42-59. doi:10.1016/j.csr.2015.06.003
DOI	10.1016/j.csr.2015.06.003
Publisher	Elsevier
Version	Version of Record
Terms of Use	http://cdss.library.oregonstate.edu/sa-termsofuse

Continental Shelf Research 105 (2015) 42–59

Contents lists available at ScienceDirect

Continental Shelf Research

journal homepage: www.elsevier.com/locate/csr

Dynamics of wind-driven estuarine-shelf exchange in the Narragansett Bay estuary

A.S. Pfeiffer-Herbert [a,*], C.R. Kincaid [a], D.L. Bergondo [b], R.A. Pockalny [a]

[a] Graduate School of Oceanography, University of Rhode Island, 215 South Ferry Road, Narragansett, RI 02882, United States
[b] U.S. Coast Guard Academy, New London, CT, United States

ARTICLE INFO

Article history:
Received 13 June 2014
Received in revised form
14 March 2015
Accepted 1 June 2015
Available online 9 June 2015

Keywords:
Wind-driven currents
Partially mixed estuary
Estuarine circulation
Inner shelf circulation
Hypoxia
Southern New England shelf

ABSTRACT

Physical exchange between estuarine and continental shelf waters impacts flushing dynamics of the estuary and determines rates of ocean inputs of nutrients and plankton. To investigate the occurrence and propagation of shelf water intrusions into the Narragansett Bay estuary, we collected velocity data near the estuarine–shelf interface during three summer periods. These data were compared to environmental forcing factors, including wind velocity, tidal mixing and river discharge. Results suggest a background cyclonic flow within the two passages of the estuary based on mean inflow in the channel on the eastern side of the estuary and mean outflow on the western shoals. Within the lower estuary this background circulation was perturbed by channel-parallel winds. On the shelf outside of the estuary, winds parallel to the coast were associated with cross-shelf flow of deep water. Strong pulses in estuarine–shelf exchange flow fell into two wind-driven modes: responses to direct forcing by down-estuary wind or rebounds following relaxation or reversal of up-estuary wind. Rebound events were common, providing the most dramatic perturbations to the mean background estuarine circulation. A reduction in exchange between Narragansett Bay and shelf waters during prevailing up-estuary winds in the summertime and short-lived pulses in exchange flow under wind reversal events are expected to affect nutrient fluxes and dynamics of hypoxia in the estuary.

© 2015 Elsevier Ltd. All rights reserved.

1. Introduction

The exchange between an estuary and continental shelf waters is a complex dynamical problem that influences ecosystem processes such as biogeochemical balances (Nixon et al., 1996; Jickells, 1998; Boehlert and Mundy, 1988) and larval transport (Boehlert and Mundy, 1988; Hare and Govoni, 2005; Tilburg et al., 2005). Wind influences circulation at the estuary–shelf interface on time scales of a few to several days (Weisberg and Sturges, 1976; Wang and Elliott, 1978; Klinck et al., 1982; Janzen et al., 2005). In this study, we examined the effects of wind forcing on exchange between estuary and shelf waters.

Wind is a dominant driver of flows on the continental shelf on synoptic time scales (Brink, 1998). In general, along-shelf wind stress drives cross-shelf surface Ekman transport on the shelf and development of a cross-shelf pressure gradient (Ekman, 1905; Allen, 1980; Brink, 1983). Interior geostrophic flow driven by the cross-shelf pressure gradient subsequently causes bottom Ekman transport opposing the surface layer transport (Allen, 1980; Weisberg et al., 2000). This balance evolves in response to the onset of wind over the course of a few inertial periods in numerical models (Li and Weisberg, 1999a; Austin and Lentz, 2002). In the inner shelf, defined alternatively as water depths where surface and bottom Ekman layers overlap (Lentz, 1995) or where bottom stress balances the bottom pressure torque due to cross-isobath flow (Weisberg et al., 2001), cross-shelf wind stress also becomes an important driver of cross-shelf transport (Li and Weisberg, 1999b; Fewings et al., 2008). Density stratification alters the cross-shelf structure and magnitude of the wind response by reducing boundary layer thicknesses, which both shifts the location of surface divergence into shallower water and strengthens the cross-shelf transports (Weisberg et al., 2000; Lentz, 2001; Austin and Lentz, 2002). The wind response may also be modified by bathymetric features that cause spatial heterogeneity in the strength of upwelling and downwelling along the coast (Brink, 1983; Weisberg et al., 2001; Castelao and Barth, 2005) and other along-shelf variability (Brink, 1991).

Estuarine circulation was traditionally viewed as a balance of the along-channel baroclinic pressure gradient and vertical mixing (Pritchard, 1956; Hansen and Rattray, 1965), but these flows are also modified by wind forcing (Weisberg, 1976; Weisberg and

* Correspondence to: Oregon State University, 104 CEOAS Administration Building, Corvallis, OR 97331, United States.
E-mail address: apfeiffer@coas.oregonstate.edu (A.S. Pfeiffer-Herbert).

http://dx.doi.org/10.1016/j.csr.2015.06.003
0278-4343/© 2015 Elsevier Ltd. All rights reserved.

Sturges, 1976). In the simple case of a narrow, laterally-uniform channel, the component of wind blowing along the axis of the channel drives near-surface water in a down-wind direction and the resulting sea surface gradient drives deeper waters up-wind (Bowden, 1953; Csanady, 1973). Observations support this basic pattern of wind-driven circulation (Pape and Garvine, 1982; Geyer, 1997; Janzen et al., 2005). Because the background gravitational circulation results in surface outflow and bottom inflow, a down-estuary wind enhances estuarine circulation and up-estuary wind stalls or reverses this background flow (Weisberg, 1976; Weisberg and Sturges, 1976).

Many estuaries are not narrow, rectangular channels, so it is important to consider how topography and rotation modify currents across an estuary. Wong (1994) developed an analytical model that extended Pritchard's (1956) momentum balances to a simple case of a channel with a triangular cross-section. Even without the influence of rotation, the model predicts that the saltier inflow from the shelf extends throughout the water column in the deepest part of the channel and the fresher outflow shifts to the shallower sides (Wong, 1994). A similar distribution of currents and salinity is observed in estuaries with approximately triangular cross sections such as Delaware Bay (Wong and Munchow, 1995) and Chesapeake Bay (Valle-Levinson and Lwiza, 1995). In estuaries with a deep channel flanked by shoals, observations and numerical models show that the wind-driven component of flow is down-wind on the shoals and up-wind in the channel (Wong, 1994; Valle-Levinson et al., 1998; Weisberg and Zheng, 2006; Narvaez and Valle-Levinson, 2008). Numerical modeling studies also demonstrate an influence of cross-channel circulation on along-channel momentum by an interaction of tides, stratification and rotation (Lerczak and Geyer, 2004; Scully et al., 2009; Li and Li, 2011, 2012). The net effect of tidal rectification and rotation is to tilt the deep inflow to the right (looking up-estuary in the Northern Hemisphere) and the outflow to the left (Huijts et al., 2009; MacCready and Geyer, 2010).

Wind also remotely influences estuary–shelf exchange by setting up sea surface elevation gradients. Through Ekman transport, an along-shelf wind that is upwelling-favorable will lower the sea level on the shelf and a downwelling-favorable wind will raise the shelf sea level relative to the estuary. The sea level gradient may then drive a barotropic response through the estuary mouth, such that upwelling conditions increase outflow and downwelling conditions increase inflow into the estuary (Wang and Elliott, 1978; Wang, 1979; Klinck et al., 1982; Wong and Valle-Levinson, 2002). There are conflicting observational and modeling results regarding the relative importance of direct and remote effects of wind on estuarine exchange. Two hydrodynamic models of estuary–shelf exchange suggest a dominant influence of remote effects by along-shelf wind forcing (Klinck et al., 1982; Garvine, 1985). Field data and an analytical model of Delaware Bay showed that currents driven by local wind forcing are up to an order of magnitude stronger than remotely-forced currents (Janzen and Wong, 2002). Observations in Chesapeake Bay, however, revealed a similar forcing magnitude between remote and local wind during strong density stratification, but remote winds dominated over local winds during periods of weak stratification (Wong and Valle-Levinson, 2002).

Here, observations of currents on the shelf and inside the lower portion of the partially-mixed Narragansett Bay estuary were used to assess the influence of wind on subtidal estuary–shelf exchange. Observations were analyzed to address three questions. First, what are the mean circulation patterns near the estuary–shelf interface of a partially-mixed estuary with complex geometry? Second, does wind forcing explain large, short-lived estuary–shelf exchange events observed in the data? Third, what are the potential impacts of the estuary–shelf exchange events on circulation and ecological processes in the estuary?

2. Study site

Narragansett Bay is a partially-to well-mixed estuary on the southern New England coastline (Fig. 1). The mid-to-lower portion of the estuary is divided into two channels with distinct topography, known as the West and East Passages. The West Passage is 4–14 km wide and 6–16 m deep, while the East Passage is slightly narrower (3–10 km) and deeper (16–48 m). Both passages have north–south trending channels flanked by a shoal on the western side. A third passage east of the East Passage, Sakonnet River, is connected by a narrow constriction that limits exchange with the rest of the bay (DeLeo, 2001) and was not included in this study. The internal Rossby radius of both the West and East passages are nearly equal to the width of each channel during the summer (Kincaid et al., 2003), making the Kelvin number ≥ 1 and indicating an importance of rotational effects.

Narragansett Bay receives water from several rivers that pass through industrialized areas. Surface freshwater input to the estuary typically ranges from 150–300 $m^3\ s^{-1}$ in the late spring to 40–65 $m^3\ s^{-1}$ in the late summer (Pilson, 1985). The estuary has fairly weak vertical stratification, with surface-to-bottom salinity differences typically less than 2 psu (Pilson, 1985) and thermal stratification appearing only in May through July (Hicks, 1959). Horizontally, the East Passage has higher salinity that the West Passage in both surface and bottom waters (Hicks, 1959). A strong influence of wind forcing on current velocities within Narragansett Bay has been reported by observational (Weisberg, 1976; Weisberg and Sturges, 1976; Kincaid et al., 2008) and modeling (Gordon and Spaulding, 1987; Bergondo, 2004; Rogers, 2008) studies. Previous shipboard surveys identified a persistent inflow on the eastern side of the East Passage and a persistent outflow on the western side of the West Passage (Kincaid et al., 2003).

Rhode Island Sound is the inner continental shelf adjacent to Narragansett Bay and bordered on the seaward side by Block Island, Rhode Island and Martha's Vineyard, Massachusetts. The depth of Rhode Island Sound has a range of 30–40 m. The inner portion of the sound has open boundaries to the south and east, but the coastline bends nearly 90° toward the south on the western side of the entrance to Narragansett Bay (Fig. 1). Rhode Island Sound is typically stratified in June through mid-September, with most of the density stratification due to a strong thermal gradient (Shonting and Cook, 1970; Rosenberger, 2001). Prior investigations suggest that summertime near-surface flow in inner Rhode Island Sound is typically west to southwestward and bottom flow is weaker and more variable (Shonting, 1969; Rosenberger, 2001; Kincaid et al., 2003).

3. Materials and methods

3.1. Data collection and processing

Time series of velocity and bottom temperature were collected by upward-looking RD Instruments Acoustic Doppler Current Profilers (ADCPs) in the late spring to summer of 2000, 2007 and 2008 (Table 1). ADCP moorings spanned the area from the inner shelf south of the estuary mouth to the mid-estuary (Fig. 1). The velocity records collected at three of the stations (SHN, EPL, WPL) in 2000 have been previously described by Rosenberger (2001) and Kincaid et al. (2008). We included these data in our analysis to extend the spatial coverage of time series information. Data collected in May–July 2000 covered the inner shelf and both passages of the lower estuary simultaneously (Table 1). The shelf mooring

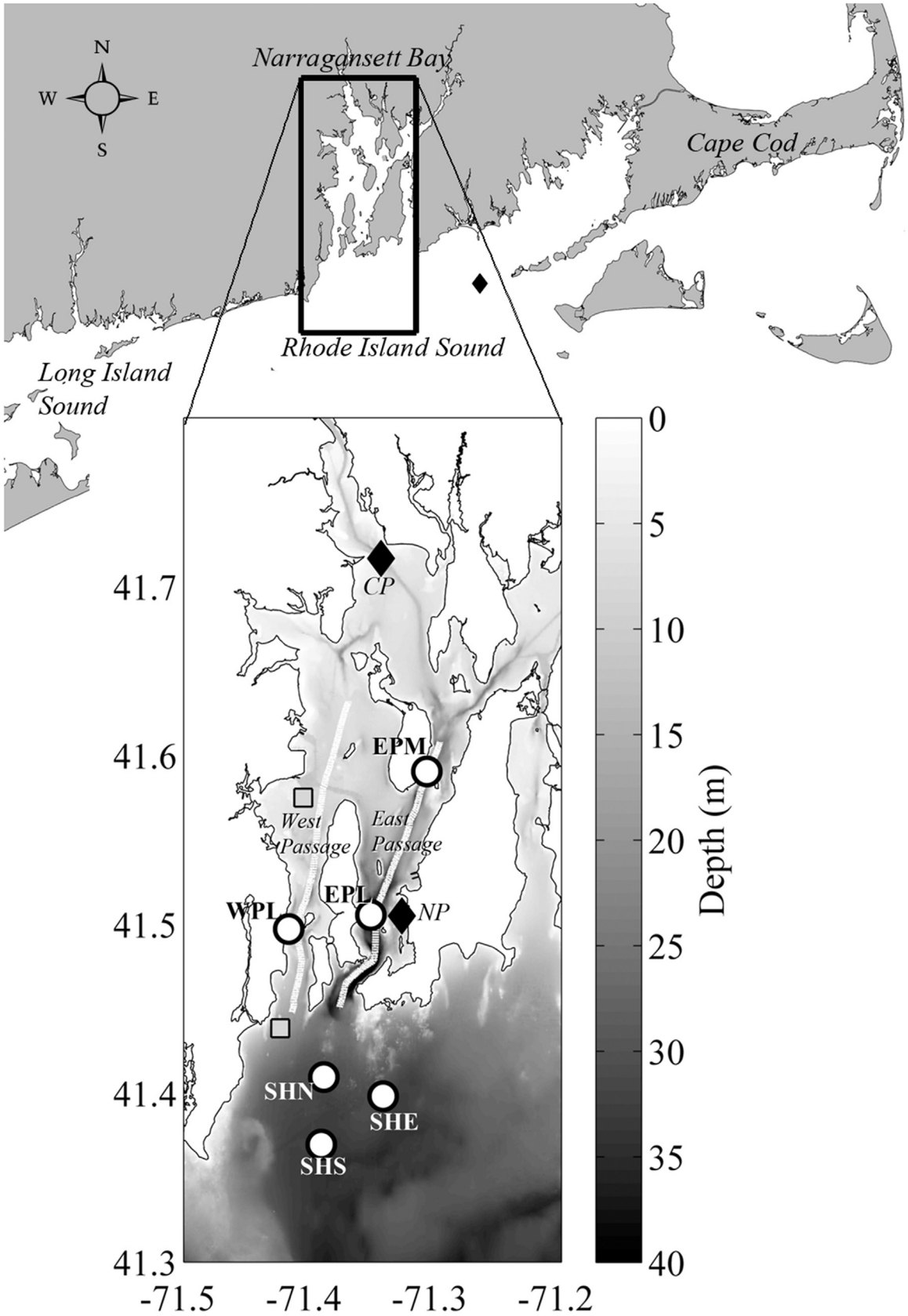

Fig. 1. Map of Narragansett Bay and Rhode Island Sound sampling stations. Large map shows location of study area on the Southern New England shelf (red box) and location of BUZM3 meteorological buoy (blue diamond). Inset map shows location of the six moored ADCP stations (red circles); year and duration of sampling are listed in Table 1. Additional data sources were meteorological and tide gauge stations (blue diamonds) at Newport (NP) and Conimicut Point (CP), vertical profiles of salinity from the GSO Fish Trawl (cyan squares) and NOAA NuShuttle surveys (yellow lines). (For interpretation of the references to color in this figure legend, the reader is referred to the web version of this article.)

Table 1
Acoustic Doppler Current Profiler (ADCP) mooring locations and sampling characteristics. Station locations are displayed in Fig. 1.

Station	Location	Depth (m)	Duration	ADCP frequency (kHz)	Bin size (m)	Good data range (m)
SHS	41°22.176′N, 71°23.448′W	33	10 July–6 October 2008	300	1	5–30
SHE	41°23.898′N, 71°20.502′W	32	10 July–6 October 2008	600	1	5–30
SHN	41°24.576′N, 71°23.322′W	30	11 May–24 July 2000	600	1	3–29
EPL	41°30.330′N, 71°21.084′W	40	21 April–6 July 2000	300	2	5–36
WPL	41°29.832′N, 71°25.002′W	12	16 May–7 July 2000	1200	0.5	2–11
EPM	41°35.436′N, 71°18.420′W	31	13 June–24 September 2007	300	1	1–28

(SHN) was 4.4 km offshore of the entrance to the estuary. The East Passage mooring (EPL) was located near the deepest parts of the channel, where dominant inflow was expected. The West Passage mooring was on the shoals to the west of the main channel to capture predominant outflow. During June–September 2007, an ADCP mooring (EPM) was installed in the East Passage channel at 17 km north of the estuary mouth. Four moorings were installed outside of the estuary mouth in an area of high bottom trawling activity in July 2008 to characterize the inner shelf circulation. Only two of these were recovered at the end of the sampling period in October 2008. The two shelf ADCP records were near the 33 m isobath, 8.8 km south (SHS) and 7.4 km southeast (SHE) of the estuary mouth.

ADCP data were quality controlled and low-pass filtered prior to further time series analysis. Velocities were recorded by the ADCPs as burst averages in 6 min intervals. Depth bins closest to the surface were omitted when more than 25% of the data were flagged as bad. Data points with error velocities greater than 3 cm s^{-1} were also removed from the time series. No more than 5 m were eliminated from the surface and no more than 4 m were eliminated from the bottom (Table 1). The percent of the water column that was missed by the ADCP ranged from 10% at Station SHN to 29% at Station WPL. Gaps in the time series of 2.5 h or less were filled by linear interpolation across each depth bin. One 5.2-h gap in the Station WPL time series was filled with the median of velocities within 6 h before and after the gap. The Station EPL time series had a 1.5 day gap, which was omitted from time averages but filled with median velocities for cross-correlation analysis. For analysis of near-surface and near-bottom velocities, data were averaged over bins at 6–8 m below the sea surface and 4–6 m above the seafloor. These depth bins were the closest to the surface and bottom, respectively, containing good data at all six stations. Finally, a 4th-order Butterworth low-pass filter with a 33-h window was applied to examine subtidal variations in the currents.

3.2. Additional data sources

Hourly wind velocity and tidal height time series were obtained from a NOAA-PORTS meteorological station at Newport, Rhode Island (41°30.3′N, 71°19.6′W) (NOAA PORTS, 2011). Additional wind velocity data were obtained from NDBC buoy BUZM3 at the entrance to Buzzards Bay, Massachusetts (41°23.8′N, 71°2.0′W) (NDBC BUZM3, 2011). Wind speed and direction were converted to eastward and northward velocity components. For comparison with subtidal currents, the wind time series were filtered with a 33-h low-pass filter. River discharge data from the Blackstone River gauge at Woonsocket, Rhode Island (USGS Blackstone, 2011) were used as an indicator of variation in freshwater input to the estuary. The Blackstone River is the largest of several rivers that enter near the head of Narragansett Bay.

Salinity data were not routinely collected as part of our study, but limited amounts of data were obtained from two sources to gain information about stratification in the estuary. The National Marine Fisheries Service conducts surveys of the East and West Passages, as well as the upper estuary, approximately once a month with a Chelsea Technologies NuShuttle undulating towed sampling platform (Narragansett Bay Window Program, 2014). We used data from two surveys coincided with our mooring time series in 2000, on 12-May and 12-June, to determine along-channel and vertical salinity gradients. A second source of salinity data was the Graduate School of Oceanography Fish Trawl Survey (GSO Fish Trawl, 2014), which conducted weekly sampling of surface and bottom salinity at a station in the mid-bay West Passage (41°34.5′N, 71°24.3′W) and the mouth of the West Passage (41°23.6′N, 71°25.4′W). These data were used to examine interannual variability in spring-summer density stratification.

3.3. Data analysis

The coordinate system at each station was defined by the principal axes of the depth-averaged flow (Fig. 2). Residual velocities were averaged by depth and then rotated to the major and minor principal component axes (Emery and Thomson, 2001). Outside of the estuary (stations SHS, SHE, SHN), the first principal axis is defined as the along-shore direction and second principal axis as the cross-shore direction. Inside the estuary (stations WPL, EPL, EPM), the first principal axis is defined as the along-channel direction and the second principal axis is defined as the cross-channel direction. For the cross-shore or along-channel direction, positive is toward the shore or head of the bay, respectively. For the along-shore or cross-channel direction, positive is roughly toward the east.

A goal of this study was to improve comparisons between fluctuations in subtidal currents and winds. Cross-covariance analysis was used to establish time-lagged relationships between the low-pass filtered wind and velocity data. Degrees of freedom were estimated by dividing the total length of each time series by the distance to the first zero-crossing of its auto-covariance spectrum (Emery and Thomson, 2001). Correlations were considered significant if they exceeded the 95% confidence interval. To find the wind directions that were most strongly related to currents, the wind velocity axes were rotated in 15° increments and cross-correlated with the along-channel or cross-shelf components of the current velocity.

Currents measured on the shelf were compared with wind velocity measured inside the estuary (NOAA PORTS, 2011) as well as wind velocity from the nearest meteorological buoy on the shelf (NDBC BUZM3, 2011) at 30 km to the East of the study site. Wind will be described throughout by the direction the wind was blowing toward (rather than the meterological convention of describing the direction wind came from) to be consistent with the oceanographic convention for water velocities. Wind velocity time series from Newport and BUZM3 had positive vector correlations (Pearson's r of 0.65–0.85) in the three years of our study (2000, 2007, 2008). BUZM3 wind was rotated counterclockwise from Newport wind on average with an offset in direction of 15–27°. The wind direction was most frequently toward the northeast (22.5–67.5°T) at both stations and in all three summers, with 33–37% of the observations falling in that direction. Correlations of

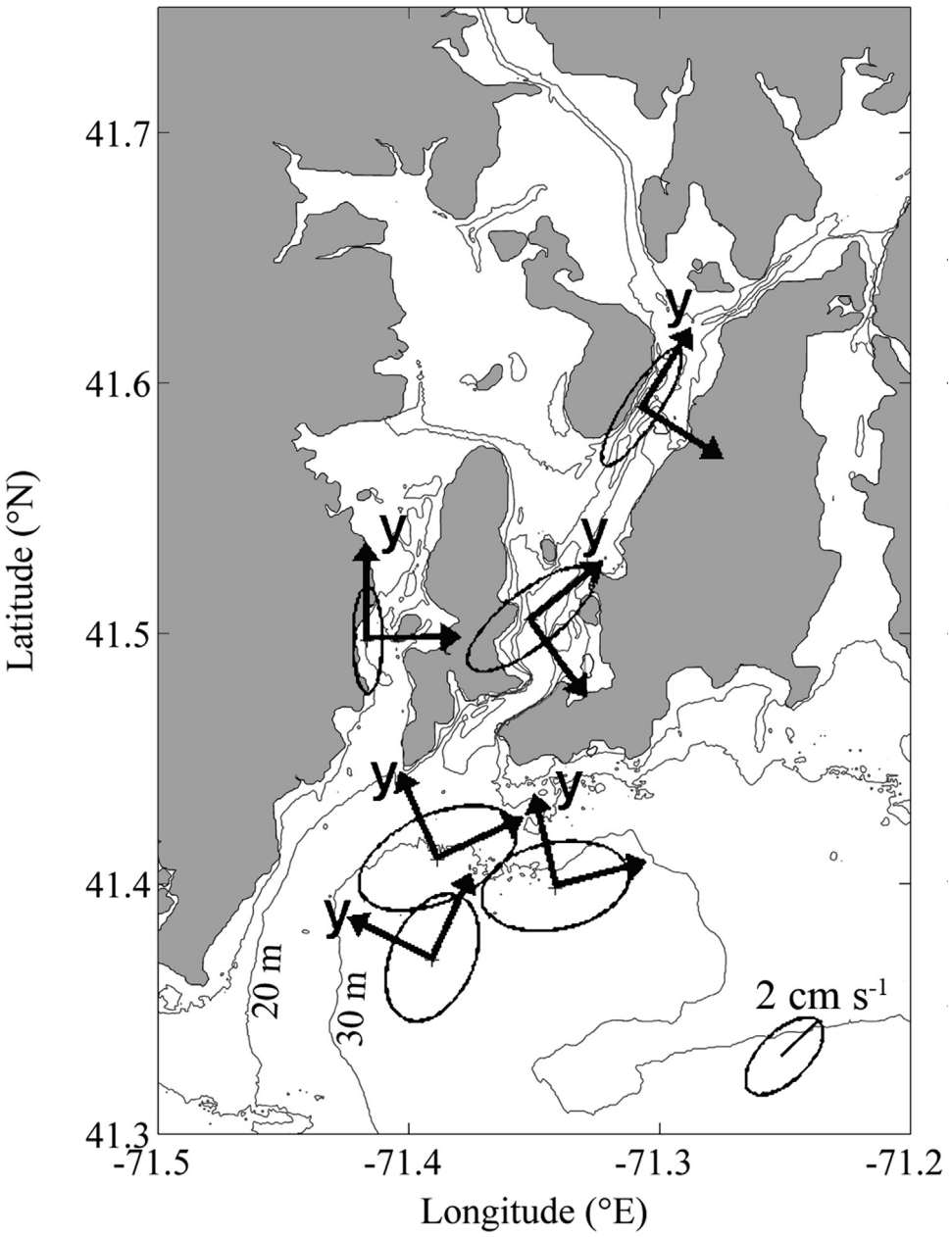

Fig. 2. Principal axes of depth-averaged subtidal velocity at each ADCP station. Size of ellipse indicates one standard deviation of the velocities. A scale ellipse with 2 cm s^{-1} major axis and 1 cm s^{-1} minor axis is shown in the lower left. Velocity data were rotated to the coordinates defined by these principal axes, where *y* is the cross-shelf or along-channel direction.

currents from shelf stations with the two wind data sources were positive over the same band of wind directions, but were stronger in magnitude for wind from BUZM3. For this reason, the BUZM3 wind time series was used for all comparisons with data on the inner shelf. Currents measured inside the estuary were compared with Newport winds for closer geographic proximity.

Near-bottom velocity time series were examined for above-average pulses in flow directed onshore (for shelf stations), up-estuary (for stations EPL and EPM) or down-estuary (for Station WPL). A velocity pulse is labeled as an enhanced exchange event if the velocity was greater than 1 standard deviation from the mean. A stalling event is defined as velocity more than 1 standard deviation below the mean. In some cases this coincided with flow that was near zero, or even reversed from its mean direction. The event duration was determined by the time that it was sustained above the 1 standard deviation limit. An event magnitude was determined for each case by integrating the velocity anomaly over the duration of the flow perturbation.

An additional goal was to characterize how background and perturbed subtidal flow compares with magnitudes of other modes of estuarine circulation. Volumetric inflow through the East Passage (Q_{EPL}) was estimated by applying the velocity profiles at Station EPL to the cross-sectional area of the channel. Velocity profiles were extrapolated to the surface by assuming constant velocity from the shallowest good bin and linearly extrapolated from the deepest good bin to zero at the seafloor as in Kirincich et al. (2005). A linear bottom profile is not the most realistic shape for the bottom boundary layer, but should not contribute much difference in total volume transport compared to applying higher order fits to velocities. A bottom boundary layer thickness of 3 m was assumed based on inspection of velocity profiles over a tide cycle. In places where the water depth was shallower than the

mooring site, velocities were linearly tapered to zero over the bottom boundary layer. Transport through the channel was calculated as

$$Q_{EPL} = \sum_{x=-L}^{L} \sum_{z=-H}^{0} v \Delta z \, \Delta x \quad (1)$$

where v is northward velocity, H is water depth and L is half of the cross-channel width centered at the deepest point adjacent to the EPL mooring site. We do not have information about the lateral velocity structure at EPL during the sampling period, but results from shipboard ADCP surveys just outside the mouth of the East Passage found that the persistent subtidal inflow covered one third of the cross-section width (Kincaid et al., 2003). At the latitude of EPL this fraction provides an L of 0.8 km over which the EPL velocity profiles were applied.

4. Results

4.1. Mean summertime velocities

Seasonally averaged currents provide a basis from which to compare shorter term fluctuations in circulation. Our velocity measurements in northern Rhode Island Sound agree with previous observations of mean westward circulation sweeping past the mouth of Narragansett Bay (Shonting, 1969; Rosenberger, 2001; Kincaid et al., 2003). Principal ellipses of the depth-averaged subtidal velocities were oriented in a northeast to southwest major axis that roughly followed the local bathymetry (Fig. 2), in contrast to tidal ellipses (not shown) which had northwest–southeast trends. Mean summertime near-surface currents were 3.7–8.6 cm s^{-1} westward to southwestward (Fig. 3). Vector correlations of currents at the two stations occupied in 2008 indicated an offset in direction of 46° near-surface and 28° near-bottom, with SHS rotated counter-clockwise from SHE similar to

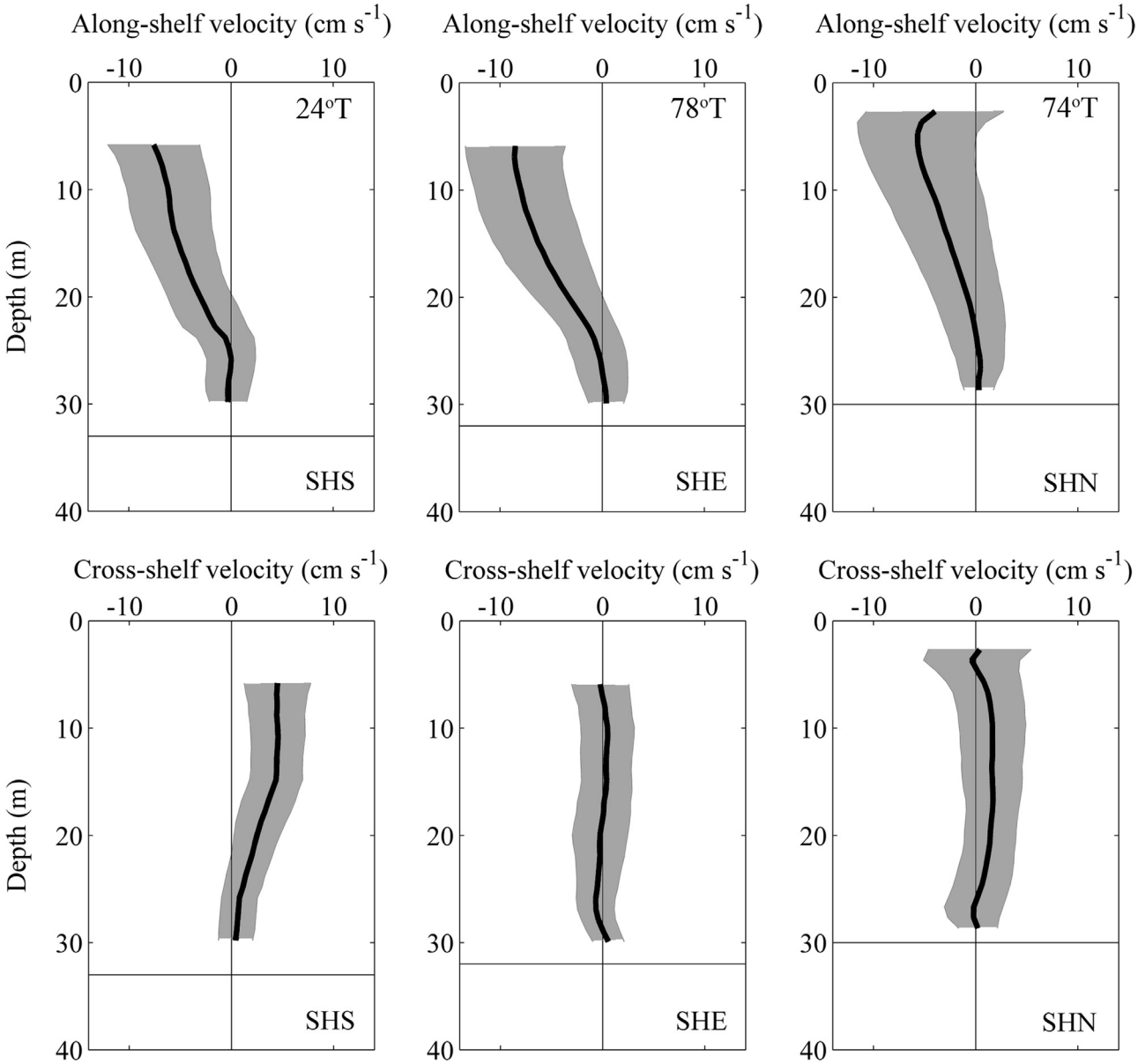

Fig. 3. Seasonally-averaged velocity profiles from moorings on the shelf. Mean (black line) and standard deviation (gray shading) of northward (upper panels) and eastward (lower panels) velocity components. Horizontal lines indicate local water depth. Major axis (along-shelf) angle of rotation shown in upper right-hand corners in degrees clockwise from north. SHS and SHE averaged over full deployment (days 192–280). SHN averaged over days 137–188.

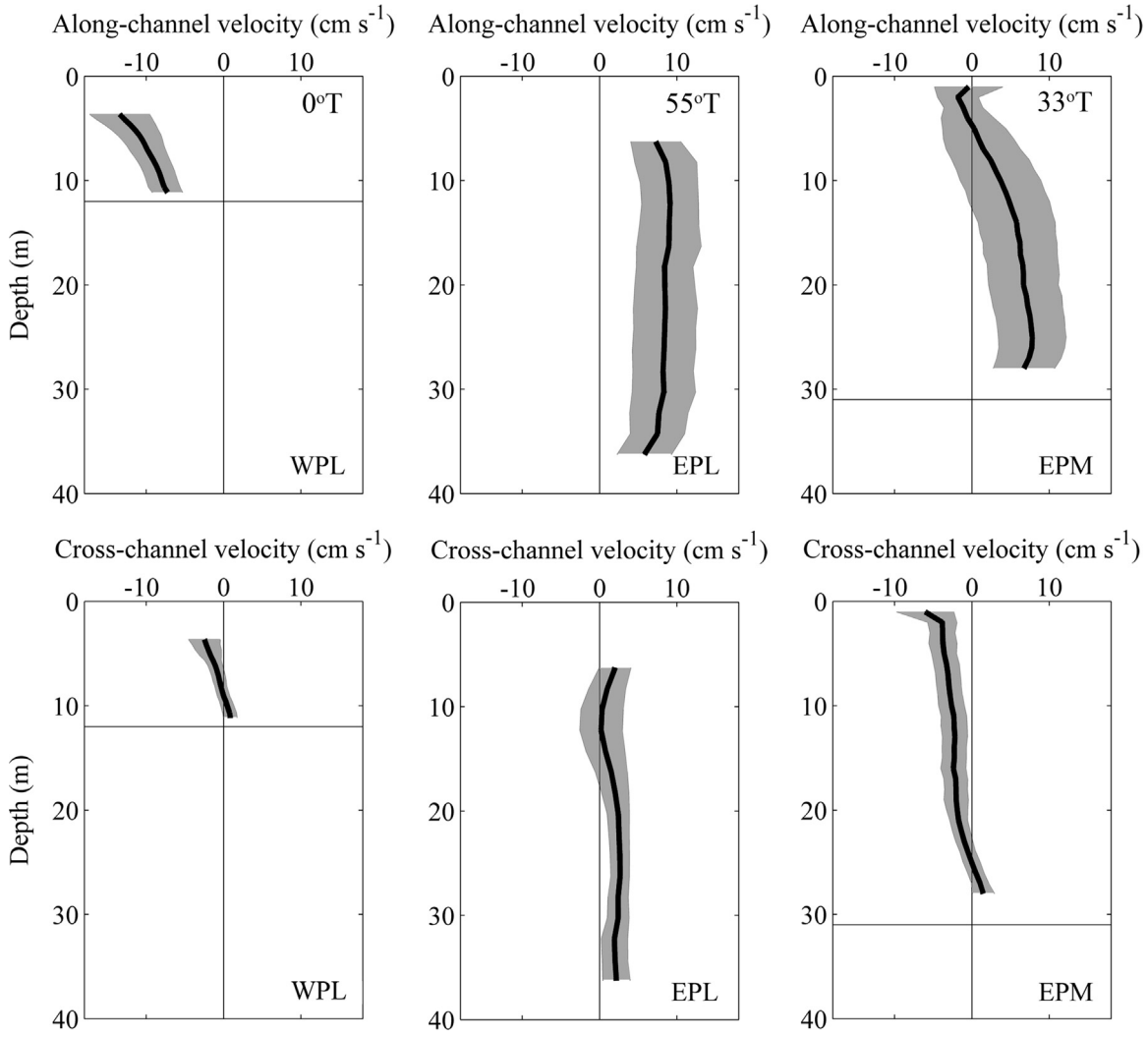

Fig. 4. Seasonally-averaged velocity profiles from moorings in the estuary. Mean (black line) and standard deviation (gray shading) of northward (upper panels) and eastward (lower panels) velocity components. Horizontal lines indicate local water depth. Major axis (along-channel) angle of rotation shown in upper right-hand corners in degrees clockwise from north. WPL and EPL averaged over days 137–188. EPM averaged over full deployment (days 164–267).

the local isobath curvature (Fig. 2). Cross-shelf flow was slower than the along-shelf flow by a factor of 2 or more. Mean near-bottom currents were an order of magnitude smaller than near-surface values. The standard deviations of cross-shelf velocity in the near-bottom layer were greater than the means (Fig. 3), indicating bottom flow was highly variable in direction. Variations in the near-bottom cross-shelf flow were used to define patterns in transport toward and away from the estuary mouth.

Mean summertime currents inside the estuary were dominated by opposing directions of inflow in the deeper channel of the East Passage and outflow on the western shoal of the West Passage (Fig. 4), in agreement with prior studies (Weisberg and Sturges, 1976; Kincaid et al., 2008; Rogers, 2008). At Station EPL in the lower East Passage, the mean along-channel velocity was up-estuary throughout the measured portion of the water column with speeds of 7.2 cm s^{-1} at 5 m below surface ("near surface") and 6.4 cm s^{-1} at 4 m above bottom ("near bottom"). At Station EPM, further up the East Passage, mean velocities were also up-estuary but increased from 1.1 cm s^{-1} near surface to near-bottom bins by to 7.8 cm s^{-1} near bottom. In bins shallower than 5 m, however, subtidal currents were 0.9 cm s^{-1} down-estuary on average at EPM (Fig. 4). There may have also been a surface layer of down-estuary flow at Station EPL, but this instrument missed the upper 5 m of the water column (Table 1). Principal ellipses of depth-averaged currents inside the estuary had higher aspect ratios than the shelf stations (Fig. 2). Tidal ellipses (not shown) were also oriented along the channels.

The average subtidal velocity at Station WPL in the lower West Passage was remarkably different from the East Passage trends, being directed down-estuary throughout the water column (Fig. 4). Because WPL ADCP was located in shallower water, it may have missed up-estuary bottom flow in the channel that was observed by Weisberg and Sturges (1976) and suggested by shipboard surveys outside of the West Passage mouth (Kincaid et al., 2003). Average speeds decreased from 13 cm s^{-1} at 3 m below the surface to 7 cm s^{-1} at 1 m above the bottom. Station WPL is much shallower that the other five stations (12 m water depth), and for consistency among stations we use depth levels near the mid-water column to represent near-surface and near-bottom currents. At these depths the mean flow was 10.5 cm s^{-1} southward. This cyclonic flow pattern between passages within the lower estuary was very consistent over time. Fluctuations in magnitude of subtidal velocity were common, but there were rarely in changes in direction (Fig. 4).

4.2. Covariance of wind and subtidal currents

Comparisons between wind velocity and cross-shelf currents

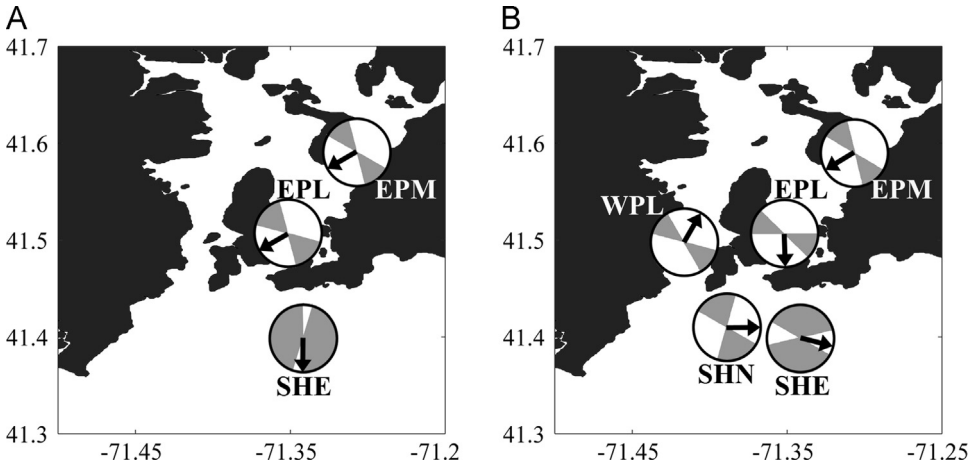

Fig. 5. Compass diagrams show the range of wind directions that were significantly correlated with (A) near-surface and (B) near-bottom currents at each station. Arrows indicate wind direction with the strongest positive correlation with cross-shelf velocity either toward shore (SHN, SHE) or along-channel velocity toward head of estuary (EPL, EPM, WPL). Gray shaded directions were not significantly correlated with the cross-shelf or along-channel flow.

revealed consistent relationships across the three shelf stations (Fig. 5). Previous analyses of cross-shelf currents at Station SHN found qualitative agreement with Ekman transport. Upwelling-favorable (eastward) wind was correlated with offshore flow near the surface and onshore flow near the bottom (Rosenberger, 2001; Kincaid et al., 2008). We extended these relationships to the two other shelf stations, SHE and SHS, which were 4 km west and 4 km south from SHN, respectively (Fig. 1). Near-surface cross-shelf flow at these sites was not well correlated with wind, except at Station SHE where near-surface cross-shelf flow was significantly correlated ($r > 0.30$, $p < 0.05$) with wind blowing toward the south (Fig. 5a). Near-surface cross-shelf flow was not significantly correlated with wind at the other two shelf stations. One explanation for why shallower circulation did not exhibit the expected wind response in our records is that the analyses did not include the shallowest 5 m of the water column (due to poor data quality in the shallowest bins), and thus likely missed the strongest wind-driven surface currents. Onshore flow near the bottom did correlate significantly ($r > 0.31$, $p < 0.05$) with wind blowing toward the east for stations SHE and SHN (Fig. 5b). The lag between wind and maximum bottom current response was up to 26 h (less than two inertial periods). The correlations between near bottom cross-shelf flow and wind at Station SHS had the same trend as the other two shelf stations, but were not statistically significant.

Comparisons of wind components and subtidal currents in the estuary also revealed consistent responses among the three estuarine records. The strength of circulation within the lower estuary varied with along-channel winds, as previously found in Narragansett Bay (Weisberg and Sturges, 1976; Kincaid et al., 2008; Rogers, 2008). The persistent deep inflow in the East Passage channel was significantly positively correlated ($r > 0.38$, $p < 0.05$) with winds blowing toward the west, southwest or south at both Station EPL and Station EPM (Fig. 5b). Along-channel near-bottom currents were most strongly correlated with southward winds (180°T; $r = 0.67$, $p < 0.05$) at EPL and southwestward winds at EPM (240°T; $r = 0.64$, $p < 0.05$). Near-surface currents were also most strongly correlated with southward winds (195°T) at EPL and southwestward winds (240°T) at EPM (Fig. 5a). In the case of the lower West Passage (Station WPL), a positive correlation in Fig. 5b with northeastward wind relates to stalling of the persistent deep outflow. Down-estuary flow at WPL was therefore significantly correlated ($r > 0.45$, $p < 0.05$) with winds blowing toward directions ranging from south–southeast through west–northwest (Fig. 5b). The down-estuary currents at WPL were most strongly correlated with southwestward wind (210°T; $r = 0.63$, $p < 0.05$). Lags between wind and currents were less than 8 h for the strongest correlations. In summary, southwestward wind was associated with strengthening of the estuarine circulation, which was up-estuary in the East Passage channel and down-estuary on the West Passage shoal.

4.3. Pulses in near-bottom subtidal velocity

The velocity time series show many brief periods of time when the deep cross-shelf or along-channel currents were considerably stronger or weaker than average (Figs. 6–8). Strong onshore and up-estuary pulses in the deep portion of the water column are consistent with a pattern of enhanced estuarine-shelf exchange. Weakening or reversal of onshore and up-estuary flow was assumed to be an indicator periods of reduced estuarine-shelf exchange.

Strong pulses in estuarine-shelf exchange flows were infrequent, making it difficult to rely on standard statistical analyses to describe the events over the 1–2 month-long deployment periods. Averaged over each time series, there was approximately one exchange event per week and events were not evenly distributed in time, but instead occurred in sporadic clusters (Figs. 6–8). During an event, the velocities were elevated by at least 1 standard deviation above the mean for an average duration of 24 h (range 1–63 h). There was no apparent trend between tidal amplitude (as a proxy for mixing) and frequency of exchange events (not shown). Events did appear to be influenced by wind (see Section 4.3.1). There was not a direct relationship with fluctuations in river discharge, but indirect effects of stratification are possible (see Section 4.3.2).

Velocity records were compared to see if near-bottom pulses were localized to a single station or widespread across more than one location. Bottom onshore pulses were commonly observed together at both of the outermost shelf stations (SHS and SHE). There were 8 on-shore velocity pulse events (60%) that co-occurred at both of these shelf stations during the 89-day records. For example, large synchronous events appeared on days 226–227 and days 251–253 in 2008 (Fig. 8b). Velocity patterns consistent with periods of enhanced exchange flows closer to the estuary–shelf interface were often localized at a single station. There were 52 days of overlap among the time series at stations SHN, EPL and WPL in 2000. Within this period of overlap there were two events in common at all three stations (Fig. 6b). The first event, on days 139–140, began with near-bottom onshore flow at Station SHN, down-estuary flow at Station EPL and weak down-estuary flow at

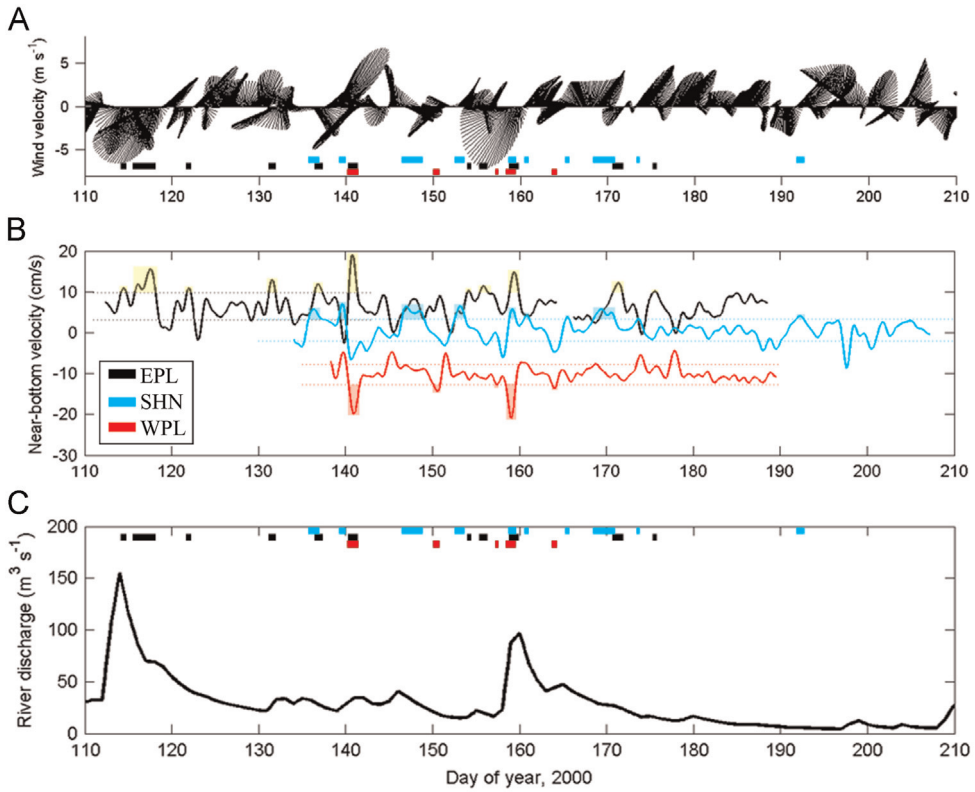

Fig. 6. Time series from summer 2000 of (A) wind velocity (m s^{-1}) at Newport, RI, (B) near-bottom cross-shelf flow (cm s^{-1}) at SHN (cyan), near-bottom up-estuary flow at EPL (black) and near-bottom down-estuary flow at WPL (red), with horizontal dashed lines at ± 1 standard deviation from mean, and (C) discharge rate of the Blackstone River (m^3 s^{-1}). Horizontal bars on (A) and (C) mark events of enhanced near-bottom currents.

Station WPL, followed by a strong rebound to up-estuary near-bottom flow at Station EPL and down-estuary flow at Station WPL. The second event, on days 158–159, first appeared as a down-estuary pulse at Station WPL followed 10 h later by strong onshore bottom flow at Station SHN and up-estuary flow at Station EPL. Four additional events at EPL coincided with bottom flow toward shore at SHN (within 40 h before the event) but no down-estuary pulse appeared at WPL.

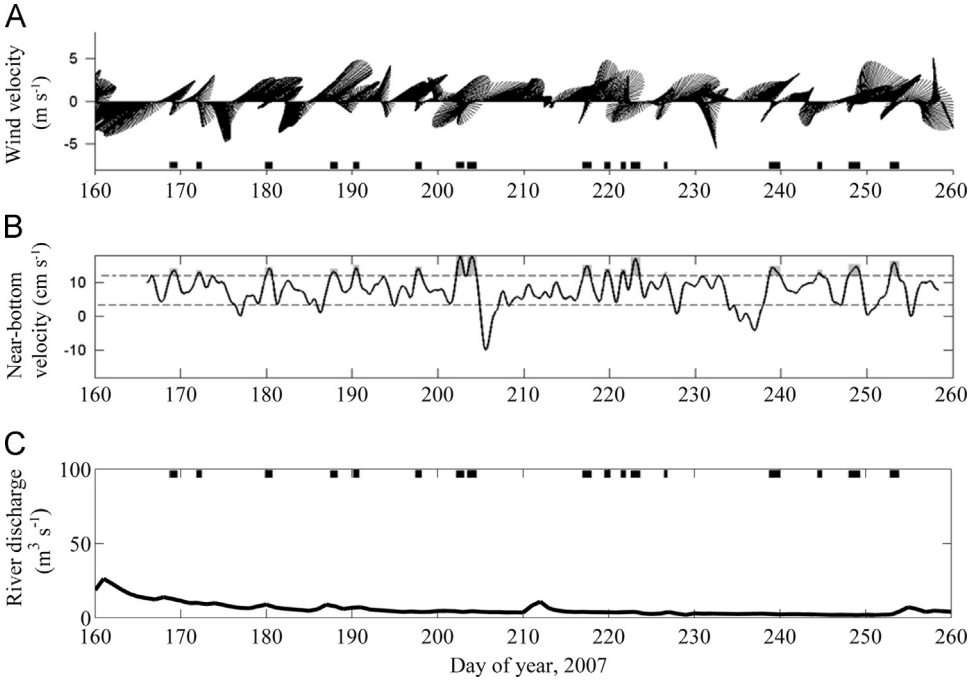

Fig. 7. Time series from summer 2007 of (A) wind velocity (m s^{-1}) at Newport, Rhode Island, (B) near-bottom along-channel flow (cm s^{-1}) at EPM in the mid-bay East Passage with horizontal dashed lines at ± 1 standard deviation from mean, and (C) Blackstone River discharge (note that the vertical scale is half of that in Fig. 6C). Horizontal bars on (A) and (C) mark events of enhanced near-bottom currents in the EPM record.

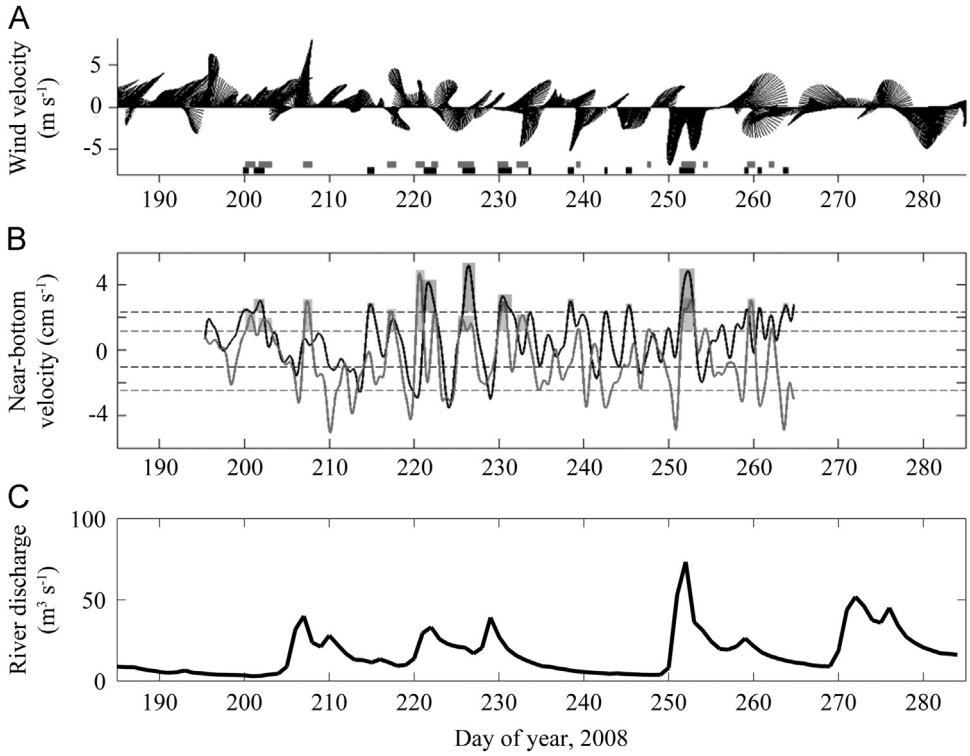

Fig. 8. Time series from summer 2008 of (A) wind velocity (m s^{-1}) at Buzzards Bay, Massachusetts, (B) near-bottom cross-shelf flow (cm s^{-1}) at SHS (black) and SHE (red) with horizontal dashed lines at ± 1 standard deviation from mean, and (C) Blackstone River discharge. Horizontal bars on (A) and (C) mark events of enhanced near-bottom currents in the SHS (black) and SHE (red) records. (For interpretation of the references to color in this figure legend, the reader is referred to the web version of this article.)

4.3.1. Effects of wind forcing

The significant relationships between wind and velocity records both in and outside the estuary suggest estuarine-shelf exchange events were also wind-influenced. The wind response of currents on the shelf will have time dependence as described in Section 1. In a two-dimensional view, the surface responds to along-shelf wind stress first to produce a cross-shelf pressure gradient, and then a bottom Ekman layer with transport opposing the surface flow develops only after interior geostrophic flow commences (Li and Weisberg, 1999b; Weisberg et al., 2000). The velocity records examined here were located in the inner shelf in a region of irregular coastline and seasonal stratification (Rosenberger, 2001); thus the wind response was not expected a priori to follow a simple two-dimensional process. Cross-covariance relationships between wind and near-bottom currents at the shelf stations were roughly consistent with the two-dimensional model, however, in that wind with a strong eastward component is expected to drive near-bottom flow toward shore.

Wind velocities before and during exchange events were categorized by the range of wind directions that were significantly positively correlated with bottom velocities at each station (Fig. 5). These are referred to as "flow enhancing winds" below. Eastward wind was determined to be a flow enhancing direction based on wind-current correlations in bottom water on the shelf, which is expected to drive onshore bottom flow. Station SHS did not have any significant correlations between wind and near-bottom cross-shelf currents, but most of the events (85%) occurred in association with wind directions that were positively correlated with onshore bottom flow at stations SHE and SHN. Station SHS had six cases (46%) where westward winds lead up to the event before switching to an eastward direction at the onset of the event. A majority of the bottom onshore events at Station SHE (60%) and Station SHN (56%) occurred in association with sustained winds that were expected to enhance onshore flow (Table 2). Strongly unfavorable wind conditions that weakened or reversed near the onset of an event were observed during 27% of events at Station SHE and 33% of events at Station SHN. The remaining a few flow perturbations at each of the shelf stations occurred during unfavorable wind conditions (Table 2).

There were two primary styles of wind forcing preceding

Table 2
Summary of near-bottom exchange event characteristics. Events were defined as periods of near-bottom flow greater than one standard deviation above the mean. Wind velocity associated with events was designated as "favorable" or "unfavorable" by correlation analysis (Fig. 5).

Parameter	SHS	SHE	SHN	WPL	EPL	EPM
"Exchange flow" direction	Onshore	Onshore	Onshore	Down-estuary	Up-estuary	Up-estuary
Threshold velocity for enhanced exchange flow	2.4 cm s^{-1}	1.1 cm s^{-1}	3.4 cm s^{-1}	12.8 cm s^{-1}	10.0 cm s^{-1}	12.0 cm s^{-1}
Number of events	13	15	9	5	11	17
Events with maximum velocity in bottom half of water column	2 (15%)	10 (67%)	9 (100%)	0 (0%)	10 (91%)	15 (88%)
Events with near-surface flow at or below average	7 (54%)	5 (33%)	8 (89%)	0 (0%)	4 (36%)	15 (88%)
Events with rebound (before or after event)	7 (54%)	11 (73%)	6 (67%)	3 (60%)	5 (45%)	9 (53%)
Events with favorable wind during event and within 6 h prior	5 (38%)	9 (60%)	5 (56%)	1 (20%)	6 (55%)	1 (6%)
Events with favorable wind during event but unfavorable wind within 6 h prior	6 (46%)	4 (27%)	3 (33%)	3 (60%)	3 (27%)	16 (94%)
Events with unfavorable wind during and within 6 h before event	2 (15%)	2 (13%)	1 (11%)	1 (20%)	2 (18%)	0 (0%)

periods of enhanced exchange flow inside the estuary: (1) sustained exchange-favorable wind prior to and during the event or (2) unfavorable winds prior to the event that shifted to a favorable direction shortly before the event. The cross-covariance relationships between wind and near-bottom currents in the lower estuary suggest that down-estuary winds, ranging from south–southeastward to west–southwestward, enhanced the average circulation pattern of deep inflow into the East Passage and outflow from the West Passage. At Station EPL, more than half of the perturbations to background flow (55%) had sustained favorable wind before and during the events (Table 2). In contrast, only 20% of events at Station WPL and 6% of events at Station EPM were associated with sustained favorable wind prior to onset. Wind conditions that shifted from unfavorable to favorable at the start of an event were common at all three estuarine stations (Table 2). Events that occurred despite unfavorable wind conditions were less common, making up 20% of the EPL and WPL cases but none of the EPM events. Perturbations to background flow during unfavorable wind conditions also had the smallest magnitudes of all identified events.

4.3.2. *Effects of river input*

Changes in freshwater input rates to the estuary affect estuarine circulation through buoyancy forcing. Density gradients, which are set by freshwater input, likely impacted the response to wind forcing (Wong and Valle-Levinson, 2002; Guo and Valle-Levinson, 2008; Jia and Li, 2012) and may have had a dominant impact on the mean estuarine circulation (see Section 5.2). Two surveys of salinity in the estuary in May and June 2000 showed stratified conditions with vertical salinity differences (excluding a 2 m layer at the surface that was not sampled) of 2.4 psu at WPL and 0.8 psu at EPL in May, and smaller inter-passage differences of 1.9 psu at WPL and 1.8 psu at EPL in June. Along-channel salinity gradients between the mouth and 16 km up each passage were $\sim$0.2 psu km^{-1} in both passages and both months, but salinity was consistently fresher in the West Passage (Fig. 9). The NuShuttle stratification patterns were on the high end of longer term observations in the West Passage (GSO Fish Trawl, 2014); in May–June of 2009–2012 there was an average surface-to-bottom salinity differences of 0.6 psu at mid-bay and 0.9 psu at the mouth, with a few observations of vertical salinity differences >2 psu. There were no significant interannual trends in salinity stratification in the Fish Trawl data, but interannual variability in river discharge patterns do occur. For example, in a 42-year period the monthly average river discharge into Narragansett Bay in April was 150 m^3 s^{-1} but varied from 50 m^3 s^{-1} to 375 m^3 s^{-1} in individual years (Pilson, 2008).

Noting the importance of river discharge in setting density patterns on longer time scales, we focus here on direct responses of subtidal exchange flow to river discharge on $\sim$1 day time scales. One caution in the interpretation of these results is that a direct river response in the estuarine circulation will not necessarily appear on these time scales, which are short compared with the estuary residence time. For example, Weisberg and Sturges (1976) discussed a requirement for time series of multiple weeks in length to distinguish non-tidal mean buoyancy circulation from wind effects in the West Passage of Narragansett Bay.

If observed pulses in near-bottom velocity were related to river discharge events, we expect a change in velocity at some delay after a peak in discharge. A previous analysis found an approximate delay of 5 days between river discharge events and the signal of these events in lower Narragansett Bay velocity records (Kincaid et al. 2008).There were two runoff events in 2000 in the Blackstone River where daily averaged freshwater flows neared 100 m^3 s^{-1} compared to background discharge rates of 10–30 m^3 s^{-1} (Fig. 6d). A larger 155 m^3 s^{-1} freshwater input occurred on day 114 that overlapped with the Station EPL record. This record had a sharp decrease in both near-surface and near-bottom velocity at 4–6 days after the river peak, suggesting that the typical up-estuary flow stalled before rebounding to slightly above average flow 7–8 days after the discharge event. The second river discharge peak of 95 m^3 s^{-1} was on day 160. Station EPL had a data gap at 4–6 days after the river discharge peak, but both near-surface and near-bottom currents were below average 7 days later. At 9 days after the peak river discharge, the near-surface and near bottom flow at EPL dropped more than one standard deviation below the mean. The Station WPL velocity record had down-estuary pulses in both the near-surface and near-bottom at 4–5

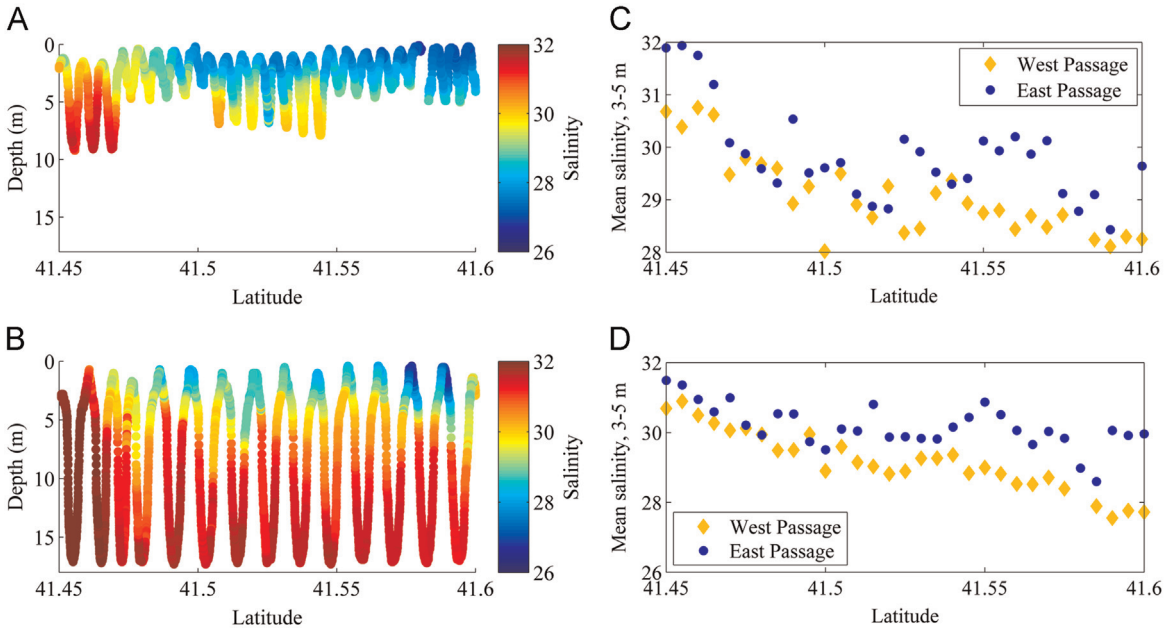

Fig. 9. Salinity profiles collected by NuShuttle along channel of the (A) West Passage and (B) East Passage on 12-May-2000. Right-hand panel shows salinity averaged over 3–5 m by latitude (mouth of the estuary is at 41.45°N) for (C) 12-May-2000 and (D) 12-June-2000. Location of these transects are shown by yellow lines in Fig. 1.

days after this discharge event. Station SHN outside of the estuary mouth had stronger offshore bottom flow at the same time as the event at WPL followed by an onshore flow event on day 165.

It is difficult to separate river versus wind forcing of events in the summertime records. The near-bottom intrusion event at Station EPL associated with a river discharge pulse was also coincident with favorable wind conditions. The down-estuary flow enhancement at WPL that followed a river discharge event occurred during unfavorable wind conditions. This suggests the freshwater input may have produced the WPL response. While river discharge may have contributed to a few of these velocity pulses, the majority of short-term near-bottom velocity pulses do not appear to be directly tied to discharge events.

Time series from the other stations had no obvious influence of river discharge on near-bottom velocity events. The Blackstone River did not exceed 25 $m^3 s^{-1}$ during the velocity sampling period in 2007 and no freshwater-related pulses in near-bottom flow were identified at Station EPM. There was one notable river discharge event in 2008. A peak 70 $m^3 s^{-1}$ runoff on day 252 coincided with a strong onshore pulse in bottom water velocity recorded at stations SHN and SHE (Fig. 8b). This event was likely a response to a change in winds rather than river flow as there was no time lag in the onset of strong bottom flow.

5. Discussion

5.1. Wind-driven modes of exchange

A goal of this study was to assess drivers of subtidal estuary–shelf exchange flows on time scales of days. Events in each of the time series that were indicative of strong exchange flows were fairly infrequent, at less than one per week, and lasted about 24 h on average. A lack of persistent patterns relating near-bottom subtidal velocity pulses to the spring-neap tide cycle or short-term variation in river runoff rule out a direct influence of these two factors on the summertime estuary–shelf exchange events on daily time scales. Wind, on the other hand, was associated with a majority of the large fluctuations in subtidal circulation. This result was not surprising because wind is a recognized driver of flows in the coastal ocean (Ekman, 1905; Csanady, 1973) and is known to be a dominant driver of subtidal fluctuations in Narragansett Bay in particular (Weisberg and Sturges, 1976; Weisberg, 1976; Rogers, 2008; Kincaid et al., 2008).

These observational records suggest that enhancements of estuary–shelf circulation occurred via two distinct styles of wind forcing. The first wind-driven mode of exchange was a local effect of along-channel wind inside the estuary. Down-estuary wind drove stronger exchange flows by enhancing background

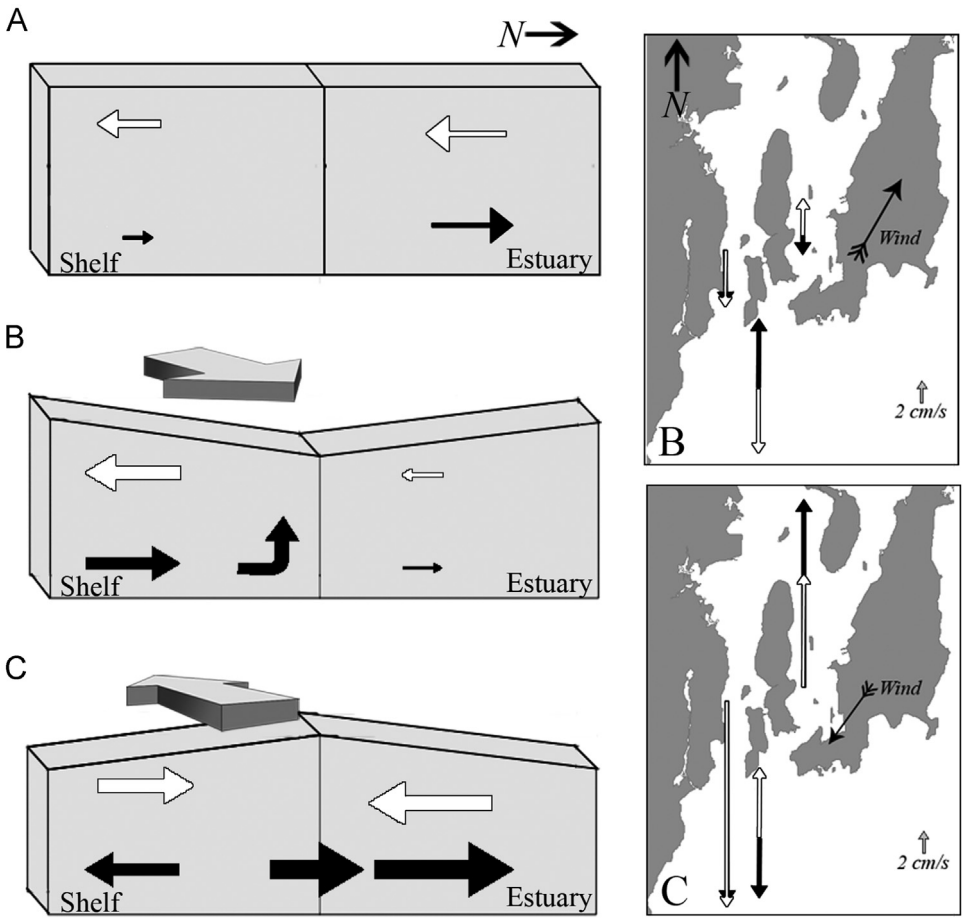

Fig. 10. Schematic of response to wind shift at estuary–shelf interface. Arrows in diagrams on left side are not to scale and the lateral structure (eastern inflow, western outflow) is simplified as vertical shear. (A) Mean circulation pattern, showing cross-shelf component on shelf and lateral structure in estuary simplified to two dimensions. (B) Wind toward northeast stalls estuarine circulation and sets up shoreward shelf bottom flow. Map view of cross-shelf/along-channel current speed near-surface (red) and near-bottom (blue) during strong northeastward wind on day 139, 2000. (C) Reversal to southwestward wind strengthens estuarine circulation and allows intrusion of shelf bottom water. Map view of cross-shelf/along-channel current speed near-surface (red) and near-bottom (blue) during strong southwestward wind on day 140, 2000. Note that during these events the cross-shelf velocity outside of the estuary is an order of magnitude larger than the mean (Fig. 3, SHN). (For interpretation of the references to color in this figure legend, the reader is referred to the web version of this article.)

gravitational circulation, while up-estuary wind stalled the background circulation. The second wind-driven mode of exchange was a two-stage process of stalling and rebounding. Because the predominant summertime wind directions were toward the northeast or southwest, winds tended to either (1) drive the deep shelf layer toward the mouth but stall the estuarine circulation or (2) strengthen estuarine circulation but drive the deep shelf layer away from the mouth. This difference in wind response regimes provides for two-stage exchange, with a potential for delivery of material in shelf waters (e.g. larvae, nutrient-rich bottom water) to a zone near the estuary mouth under northeastward winds followed by a draw-in of material when the wind shifts to southwestward.

5.2. Subtidal momentum balances

The schematic of wind response in Fig. 10 implies Ekman upwelling and downwelling on the shelf outside of the estuary mouth, with a dominant balance between along-shelf wind stress and rotation. This balance omits other important dynamics affecting sea surface elevation outside the estuary mouth, however, which could explain the fairly low correlation ($r^2 \leq 0.4$) between cross-shelf velocities and wind stress. Surface and bottom boundary layer interaction is likely given the 30–35 m water depths of the moorings, affecting the Ekman balance by increasing importance of bottom stress (Lentz et al., 1999; Weisberg et al., 2005; Lentz and Fewings, 2012). Propagation of coastal-trapped waves, a more remote effect of atmospheric forcing, also causes oscillations in the sea level at the coast that will influence transport through the estuary mouth (Gill and Schumann, 1974; Janzen and Wong, 2002; Wong and Valle-Levinson, 2002). Finally, summertime density stratification and possible upslope mixing of bottom water near the mouth of the East Passage (Kincaid et al., 2003) could further affect the estuary–shelf interaction. In all of these cases, the qualitative relationship in Fig. 10 between wind and changes in cross-shelf sea level on the shelf remains, which provides a sea level boundary condition at the mouth of the estuary.

Inside the estuary, Fig. 10 implies a balance of along-channel (y-direction) pressure gradient and vertical (z-direction) stress divergence for the subtidal momentum as in Pritchard (1956)

$$K_z \frac{\partial^2 v}{\partial z^2} = -\frac{g}{\rho_o}\frac{\partial P}{\partial y} \tag{2}$$

where K_z is the vertical eddy viscosity, v is along-channel subtidal velocity, ρ_o is a reference density and P is pressure. This is a great simplification, as it is well-known that density and eddy viscosity are not spatially or temporally constant in estuaries (Jay and Smith, 1990; Simpson et al., 1990; Whitney et al., 2012; Geyer and MacCready, 2014). Acknowledging the real-world complexity, it is useful to examine simple momentum balances to see where these do or do not agree with the observations. Winant (2004) presented an analytical model for the response to wind stress in a basin without density stratification using the momentum balance in Eq. (2) with the addition of rotation. Narvaez and Valle-Levinson (2008) applied the Winant (2004) model to a shallow estuarine channel by neglecting rotation, providing a non-dimensional solution of

$$v^* = \frac{\partial \eta^*}{\partial y^*}\left(\frac{z^{*2} - h^*}{2}\right) + (z^* + h^*) \tag{3}$$

where the non-dimensional variables are along-channel velocity ($v^* = \frac{\rho K_z}{\tau H} v$) with water density ρ, vertical eddy viscosity K_z and along-channel wind stress τ; sea surface height anomaly ($\eta^* = \frac{\rho g H}{\tau L}\eta$); along-channel distance ($y^* = \frac{y}{L}$) compared to estuary length L; vertical distance ($z^* = \frac{z}{H}$) compared to dimensional water depth $H(x)$, and water depth ($h^* = \frac{H(x)}{H_{max}}$). Requiring zero net volume transport through the cross-section, the sea level gradient can be approximated by $\frac{\partial \eta}{\partial y} = \frac{3}{2}\frac{\langle h^{*2}\rangle}{\langle h^{*3}\rangle}$, with angle brackets indicating cross-sectional averages of water depth (Narvaez and Valle-Levinson, 2008).

The simplified balance in Eq. (3) assumes barotropic pressure gradient forcing caused by sea surface elevation gradients, which we assessed with observations. Surface elevation slopes were obtained from tide gauge data at three NOAA PORTS stations (Conimicut, Quonset, Newport). The sea level time series from individual stations were processed before intercomparison by subtracting annual mean sea level from the sea level time series and low-pass filtering to remove tides. An inverse barometer correction was applied as in Gill (1982) using atmospheric pressure data from the same stations. Surface elevation anomalies at head of the bay (Conimicut Point; Fig. 1) were compared with surface elevations in the mid-bay West Passage (Quonset Point) and lower bay East Passage (Newport). The sea level slopes were highly coherent among the three stations during the time frame shown in Fig. 6. There was also strong coherence between sea level slope and along-channel wind (Fig. 11). There are a few clear examples that support the conceptual model that along-channel wind sets up the sea surface toward the head or mouth of the estuary, driving a barotropic response in the bottom layer of the East Passage and enhancing or stalling the estuarine exchange flow (Fig. 11). Up-estuary wind on day 139 corresponded with an up-estuary sea surface slope and near-bottom velocities that reversed at EPL and stalled at WPL. The wind reversal on day 140 and similar strong

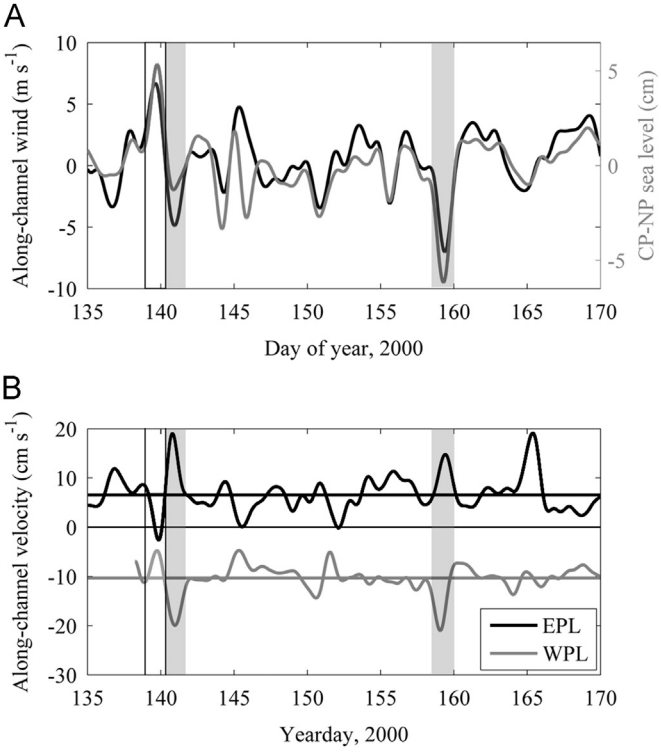

Fig. 11. (A) Along-channel wind (black; positive toward head of estuary) and sea level difference between Conimicut Point and Newport (red). (B) Subtidal near-bottom velocity from stations EPL and WPL with horizontal lines at mean velocity. Shaded bars highlight stalling event on day 139 (purple) and enhanced exchange events on days 140 and 159 (green). (For interpretation of the references to color in this figure legend, the reader is referred to the web version of this article.)

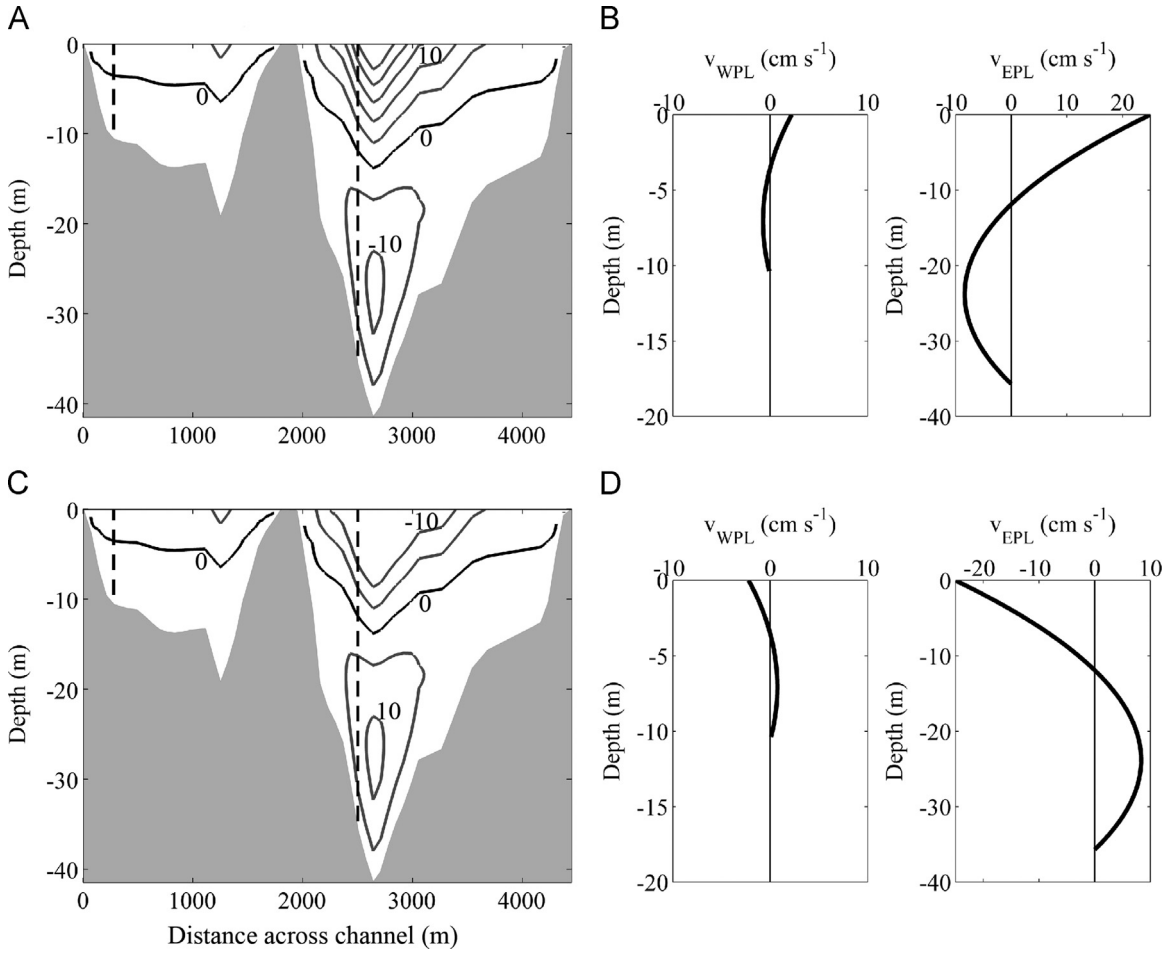

Fig. 12. Results of Eq. (2) analytical model for wind-driven along-channel velocity (v) with K_z of 1.5×10^{-3} m^2 s^{-1} and wind stress of ± 0.05 Pa. (A) Cross-section of v versus depth under up-estuary wind stress of 0.05 Pa. (B) Profiles of v at location of WPL and EPL (vertical dashed lines in (A)) for up-estuary wind. (C) Cross-section of v versus depth under down-estuary wind stress of -0.05 Pa. (D) Profiles of v at location of WPL and EPL for down-estuary wind. Note that in the cross-section views the distance between the two passages was shortened by removing land.

down-estuary wind on day 159 corresponded to the reverse effect; sea surface sloped upward toward the estuary mouth and the exchange flows strengthened.

A key difference between the two passages in the lower portion of Narragansett Bay is that the maximum water depth is much larger in the East Passage. This makes the East Passage naturally a conduit for most of the inflow of bottom water from the shelf into the bay (Hicks, 1959; Kincaid et al., 2003), as well as affecting cross-estuary flow between the passages due to differential sea surface set-up (Weisberg and Sturges, 1976). We applied Eq. (3), which considers along-channel velocity as a function of water depth, to a bathymetric cross-section of Narragansett Bay at 41.5°N (near the WPL and EPL sites) assuming a representative ρ of 1022 kg m^{-3} from NuShuttle survey data and selecting K_z of 1.5×10^{-3} m^2 s^{-1} to best match the maximum EPL bottom layer velocity anomalies during strong wind events of $\sim$10 cm s^{-1}. The results for wind stress of ± 0.05 Pa (equivalent to wind events on days 139–140, 2000; Fig. 6) are shown in Fig. 12.

The analytical model (Eq. (3)) predicts dominant wind-driven exchange flows in the East Passage and muted response in the West Passage (Fig. 12). A similar contrast in summertime subtidal inflow and outflow volume transports through the East versus West passages was observed by Kincaid et al. (2003) in shipboard ADCP surveys conducted just outside the mouth of each passage. The shipboard sections, however, showed isotachs tilting down toward the west, such that the inflow was shifted to the east and outflow to the west side of the passages. This type of lateral structure, which differs from the classic two-layered estuarine circulation, has been noted elsewhere with effects of rotation and cross-channel variation in bathymetry invoked to explain the lateral tilting (Wong and Munchow, 1995; Valle-Levinson et al., 1998; Li and Li, 2012). The internal Rossby radius near the estuary mouth was on the same order as the width of each passage ($\sim$4 km), allowing for an influence of rotation (Kincaid et al., 2003).

Another contrast between the analytical model of wind response and observations in the lower estuary passages is that the time series of velocity presented in this study had mean outflow on the west side of the West Passage that was similar in magnitude to, rather than significantly smaller than, mean inflow in the deeper channel of the East Passage. An important term neglected in Eq. (3) is the influence of density stratification, which is typically a dominant driver of exchange flow in estuaries (Dyer, 1997; MacCready and Geyer, 2010). The Knudsen (1900) relation estimates exchange flow from freshwater discharge and the vertical salinity difference at the estuary mouth. This relation provides an upper bound to buoyancy-driven transport in a two-layered, steady state scenario (Pawlowicz, 2001; MacCready and Geyer, 2010), which differs from the weaker density stratification and time-varying wind forcing present in Narragansett Bay. Nevertheless, estimates of buoyancy-driven transport at the mouth of each passage are as follows. Salinity profiles collected on 12-June-2000, when freshwater discharge from the 8 major rivers combined was approximately 150 m^3 s^{-1}, had vertical gradients of 1.9 and 1.8 psu in the West and East passages, respectively.

Assuming that the freshwater content divides evenly among the two passages (which is not entirely realistic because the lower West Passage was about 0.4 psu fresher than the East Passage), the expected inflow and outflow volumes were similar in the two passages. The West Passage had predicted inflow volume transport of 1.25×10^3 m^3 s^{-1} and outflow of 1.18×10^3 m^3 s^{-1}, while the East Passage had predicted inflow of 1.33×10^3 m^3 s^{-1} and outflow of 1.26×10^3 m^3 s^{-1}. These results highlight an important clarification that the wind-related pulses in the observed velocity records are on top of a mean inflow/outflow pattern that is likely governed by seasonal stratification patterns. Furthermore, complex interactions between wind and density fields could affect both the magnitude of exchange and lateral structure as described in a number of modeling studies (e.g., Guo and Valle-Levinson, 2008; Chen and Sanford, 2009; Li and Li, 2011, 2012).

The Wedderburn number (Monismith, 1986) has been applied to estuaries to compare the strength of wind and buoyancy effects on circulation (Geyer, 1997; Chen and Sanford, 2009). This non-dimensional parameter is defined as $W = \frac{\tau_w L}{\Delta\rho g h^2}$, where τ_w is the along-channel wind stress, L is the along-channel length scale, $\Delta\rho$ is the along-channel change in density, g is gravitational acceleration and h is the vertical length scale (water column or layer thickness). Measurements of density from the two NuShuttle surveys (yellow lines in Fig. 1), in May and June 2000, were used to calculate W in the lower estuary passages for the portion of the water column below the pycnocline. The along-channel density gradients in May were 0.2 kg m^{-3} km^{-1} in the West Passage and 0.03 kg m^{-3} km^{-1} in the East Passage, but a difference in h makes W approximately equal between the passages. The June survey had similar $\Delta\rho$ and equality of W between the passages. Extrapolating from density gradients measured in the two surveys, an along-channel wind stress of approximately 0.08 Pa, equivalent to 7.5 m s^{-1}, was required for $W=1$. Maximum winds associated with the two widespread exchange events in 2000 (days 139 and 159; Fig. 6) exceeded that threshold, indicating a dominance of wind forcing in the estuarine circulation. These measurements produce $W \ll 1$ during low winds, such as the time of the NuShuttle survey in May (day 133), underscoring the episodic nature of wind-driven circulation above a more slowly varying buoyancy circulation.

5.3. Impact of subtidal exchange events

Significant estuary–shelf exchange can be inferred for periods when enhanced estuarine inflow corresponded with deep shelf currents flowing toward the estuary mouth. In 2000, when data were collected simultaneously on the shelf and in both passages of the estuary, most of the periods of strong estuarine flows or onshore flow on the shelf were localized to a single station. One large event appeared in data from all three stations. This large-scale estuary–shelf exchange event occurred on days 139–140 (Fig. 6) and represents an excellent example of a two-stage shelf to estuary intrusion process. As depicted in the schematic in Fig. 10B, the event began during a northeastward wind, with strong onshore flow at the shelf station and stalled flow at both estuarine stations. As the wind shifted to southwestward, the estuarine circulation rebounded with strong inflow in the East Passage channel and outflow on the West Passage shoal (Figs. 6B and 10C). The near-bottom current on the shelf, meanwhile, turned to an offshore direction (Fig. 6B).

Although the event on day 140 was only one of two widespread events observed in the early summer of 2000, the wind conditions during this period are relatively common in summer. In June through August of 2000 and 2007, the wind shifted from strongly unfavorable (i.e. directed up-estuary with speed greater than 1.6 m s^{-1}) to strongly favorable 20 times, or approximately every 5 days. Not all of the wind shifts resulted in up-estuary flow enhancement in the East Passage. Roughly 40% of these characteristic wind shifts were not associated with an event during the sampling periods at either EPL or EPM (Figs. 6 and 7). Velocity data were not collected on the shelf or lower estuary while the EPM station was operational, but two events observed at this mid-bay station with similar characteristics to the widespread event on day 140 of 2000. The two up-estuary pulse events at Station EPM, on days 238 and 253 in 2007, began with stalled flow during strong northeastward winds followed by a strong rebound after the wind shifted toward the southwest (Fig. 7). Given the similarities to the day 140 event (in 2000) at Station EPL, it is likely that these two up-estuary pulses in 2007 were also a widespread strengthening of estuary–shelf exchange.

If strong pulses in estuary–shelf exchange occur only a few times each summer, it is important to consider whether such events impact estuary flushing. Numerical modeling experiments simulating Narragansett Bay found large variations in residence time of sub-estuaries of the upper bay in relation to wind direction (Rogers, 2008). One method of estimating flushing time is as the ratio of estuary volume to volume transport rates (Monsen et al., 2002). This is a simplistic view of flushing in an estuary with complex geometry and non-steady state conditions, but it indicates the relative contribution of exchange flow at the estuary mouth. Estimated inflow in the lower East Passage channel (Q_{EPL}, Eq. (1)) was large relative to average and perturbed freshwater input from rivers. Mean Q_{EPL} was 0.9×10^3 m^3 s^{-1} over the full time series. Q_{EPL} was 1.5×10^3 m^3 s^{-1} on average during events and up to 2.3×10^3 m^3 s^{-1} for the largest intrusion event. Compared with the volume of the estuary of 2350×10^6 m^3 (excluding Providence River, Mount Hope Bay and Sakonnet River; Pilson, 1985), the mean flow suggests an apparent residence time of 30 days, similar to Pilson's (1985) estimate of monthly average residence times of 19–33 days in early summer. The estimated volume transport during events reduces apparent residence times to 12–18 days, or approximately half of the seasonal average. Note, however, that the enhanced exchange events were considerably shorter in duration than these residence times (days versus weeks), and thus the actual impact on residence time would be smaller.

Another metric for intrusion event impact is the net excursion obtained by integrating velocity over the duration of the events. Estimating excursion distances from velocity at a single point is admittedly problematic because the velocity field may change dramatically over distances smaller than the implied excursions. We restrict this analysis to two locations: (1) shoreward flow at SHN where shipboard velocity data collected closer to the estuary mouth (Kincaid et al., 2003) suggest that a continuation of flow into the estuary is plausible, and (2) the East Passage where two current records had mean up-estuary flow in the channel and similar wind response in the lower and middle estuary (Figs. 6 and 7). Pulses in cross-shelf bottom flow toward the estuary mouth at SHN had excursion lengths greater than the distance to the mouth in 44% of the events. Near-bottom up-estuary pulses at EPL had excursion lengths of 3–26 km. We estimate 64% of these excursions exceeded the 7 km distance from the estuary mouth to the EPL site. Only one event had an excursion length that extended as far as Conimicut Point at the head of the bay (Fig. 1). Most excursion lengths estimated for WPL (e.g. 6–19 km) were sufficient to allow water parcels to exit the estuary mouth. The mid-estuary velocity record at EPM had excursion lengths of 2–15 km, with 17% of these exceeding the distance to the entrance to the urban-impacted Providence River at Conimicut Point. Length scale estimates for near-bottom velocity pulses suggest that several periods could reasonably result in subtidal transport between the mouth and the

lower/mid estuary sites. The largest events appear to be capable of transporting water into the upper estuary.

Some of the inflow at EPL and outflow at WPL may pass through a break between islands at 41.57°N or turn within the passages and not extend into the upper estuary. Analysis of West Passage currents by Weisberg and Sturges (1976) suggested communication between the passages influenced the response time to wind events, for example. Our observations cannot distinguish such flows directly, but there is evidence that a sizable portion of the inflow of shelf water does propagate further into estuary and contribute to material exchange. First, fluctuations in bottom velocity at EPM, north of the break between the islands, had a similar relationship to along-channel wind as at EPL. By conservation of mass these mid-estuary events must draw water from the lower estuary, and the excursion lengths described above suggest that it comes from as much as 15 km away. Secondly, the West Passage channel had higher freshwater content compared to the East Passage inflow. Salinity measured by NuShuttle surveys decreased from the East Passage to the West Passage and in particular the sub-halocline salinity (below 5–8 m) remained within 0.5 psu of the bottom salinity at the mouth for more than 10 km into the East Passage. Salinity consistent with shelf water only appeared in the first ~2 km of the West Passage (Fig. 9). These salinity observations support the concept of predominant East Passage inflow and West Passage outflow extending into the mid-estuary rather than net inflow/outflow turning within each of these physically separated passages of the lower estuary.

5.4. Implications for hypoxia

One ecosystem process of concern in Narragansett Bay is summertime hypoxia (Bergondo et al., 2005; Deacutis et al., 2006; Codiga et al., 2009). Hypoxia in estuaries is linked to high nutrient loads that fuel high biological productivity and supply the organic matter necessary for oxygen draw-down (Diaz, 2001; Kemp et al., 2009). A key component of this cycle is the retention of nutrients and organic matter in high enough concentrations to impact oxygen levels before the water is ventilated by vertical mixing or lateral advection (Kemp et al., 2009). Upper Narragansett Bay waters have indicators of excess nutrients, including blooms of phytoplankton and macroalgae and loss of historic seagrass beds (Deacutis, 2008). Likewise, the upper reaches of Narragansett Bay are commonly suboxic (dissolved oxygen less than 4.8 mg L^{-1}) and episodically hypoxic (dissolved oxygen less than 2.9 mg L^{-1}) in July and August of each year (Saarman et al., 2008).

Rates of exchange between the estuary and shelf waters may affect ecosystem dynamics such as hypoxia by setting residence times within the estuary (Dyer, 1997). Results of this study confirmed that prevailing summertime winds suppress estuarine-shelf exchange in Narragansett Bay. With lower river discharge compared to winter–spring (Pilson, 1985) and decreased wind-driven exchange flow, the physical conditions in the summertime likely allow additional build up of organic matter in the estuary by increasing residence time. Apparent residence times were reduced by half during wind reversals compared with the mean conditions. The wind-related slow down of flushing is specific to the geography of this estuary; estuaries with a different shelf and channel orientation relative to prevailing winds, such as Delaware Bay on the U.S. east coast (Goodrich, 1988), may not experience the same effect.

Hypoxia in bottom waters of the upper estuary typically persists for one to several days (Codiga et al., 2009), similar to time scales of wind fluctuations. Wind-driven exchange events in the lower bay have the potential to relieve hypoxic conditions by advection of oxygenated bottom waters up into the estuary as indicated by excursion lengths > 10 km in largest East Passage intrusion events. Alternatively, intrusion of shelf waters could exacerbate the conditions for hypoxia by contributing nutrients that fuel primary production. A nutrient budget for Narragansett Bay estimated that Rhode Island Sound supplies about 20% of the total dissolved inorganic nitrogen (DIN) to the estuary annually, with rivers and wastewater contributing the majority of DIN (Nixon et al., 1995). Earlier work suggested that periodic diatom blooms in the summertime exceed the productivity expected from known sources of DIN at that time of year (Furnas et al., 1976; Chaves, 2004). It is possible that, as speculated by Nixon et al. (1995), large volume exchange events at the mouth supply the nutrients needed. Our observations of estuary–shelf exchange following wind conditions favorable for upwelling of shelf waters support this hypothesis.

Statistical models of Narragansett Bay hypoxia at the event scale do not explain much of the variance in the hypoxic episodes (e.g. Codiga et al., 2009), which is not surprising given the complex interactions of the physical and biological factors involved. Wind-driven fluctuations in estuary–shelf exchange, and subsequent advection and mixing of water masses, must be a factor in the dynamics that control hypoxia in the estuary. How the exchange events propagate into the impacted waters of the upper estuary remains to be determined.

6. Conclusions

Exchange between the Narragansett Bay estuary and adjacent shelf waters appeared to be strongly influenced by wind forcing, as suggested by previous studies (Weisberg and Sturges, 1976; Kincaid et al., 2008). Winds blowing toward shore and in an upwelling-favorable direction promoted deep flow from the inner shelf toward the mouth of the bay, but these winds were significantly correlated with stalling the deep inflow in the East Passage. Winds blowing down-estuary were favorable for enhancing deep exchange flow in the lower estuary, but these wind directions were also significantly correlated with offshore bottom flow at the inner shelf stations. The relationships between wind and currents suggest that intrusion of shelf water into Narragansett Bay is often a two-stage process rather than a direct wind response driving the deep shelf waters into the estuary. A conceptual model of this process is that prevailing summertime winds toward the northeast first allow shelf water to build up at the mouth of the estuary. Then, when prevailing wind conditions relax or reverse, a pulse of shelf water enters the East Passage of the estuary accompanied by strengthened outflow from the West Passage.

Periods of enhanced deep exchange flow may improve water quality in the estuary by shortening the flushing time. In six current velocity records, we observed several pulses per month of elevated near-bottom velocity from the shelf stations toward shore, up the East Passage or down the West Passage of the estuary. A majority of these estuary–shelf exchange pulses coincided with relaxation from unfavorable wind velocity, supporting the idea of a two-stage intrusion process. Other pulses occurred as slow increases in flow during sustained down-estuary winds. These relatively short-lived, strong pulses in exchange likely affect nutrient concentrations and related ecosystem processes in partially-mixed estuaries in a way that is not captured by mean transport or bulk methods of calculating estuarine flushing rates.

Acknowledgments

Funding for this research was supplied by Rhode Island Sea Grant, University of Rhode Island (Grant #NA86RG0076), NOAA

Coastal Hypoxia Research Program (Grant #NA05NOS4781201), and Rhode Island Natural History Survey (John Wald Science Grant, 2008). This paper was greatly improved by the suggestions of three anonymous reviewers. We thank everyone who assisted with field work and data processing, especially Kurt Rosenberger, Justin Rogers, and Andrew Sayre. The captains and crew of the R/V Cap'n Bert and R/V Beavertail are also gratefully acknowledged.

References

Allen, J.S., 1980. Models of wind-driven currents on the continental shelf. Annu. Rev. Fluid Mech. 12, 389–433.
Austin, J.A., Lentz, S.J., 2002. The inner shelf response to wind-driven upwelling and downwelling. J. Phys. Oceanogr. 32, 2171–2193.
Bergondo, D., 2004. Examining the Processes Controlling Water Column Variability in Narragansett Bay: Time Series Data and Numerical Modeling (Ph.D. thesis). University of Rhode Island, Kingston RI.
Bergondo, D., Kester, D., Stoffel, H., Woods, W., 2005. Time-series observations during the low sub-surface oxygen events in Narragansett Bay during summer 2001. Mar. Chem. 97, 90–103.
Brink, K.H., 1983. The near-surface dynamics of coastal upwelling. Prog. Oceanogr. 12, 223–257.
Brink, K.H., 1991. Coastal-trapped waves and wind-driven currents over the continental shelf. Annu. Rev. Fluid Mech. 23, 389–412.
Brink, K.H., 1998. Wind-driven currents over the continental shelf. In: Brink, K.H., Robinson, A.R. (Eds.), The Sea, volume 10. Wiley, Chichester UK, pp. 3–20.
Boehlert, G., Mundy, B., 1988. Roles of behavioral and physical factors in larval and juvenile fish recruitment to estuarine nursery areas. American Fisheries Society Symposium, vol. 3, pp. 51–67.
Bowden, K., 1953. Note on wind drift in a channel in the presence of tidal currents. Proc. R. Soc. Lond. Ser. A: Math. Phys. Sci. 219, 426–446.
Castelao, R.M., Barth, J.A., 2005. Coastal ocean response to summer upwelling favorable winds in a region of alongshore bottom topography variations off Oregon. J. Geophys. Res.: Oceans 110, C10S04.
Chaves, J., 2004. Potential Use of ^{15}N to Assess Nitrogen Sources and Fate in Narragansett Bay (Ph.D. thesis). University of Rhode Island, Kingston RI.
Chen, S.N., Sanford, L.P., 2009. Axial wind effects on stratification and longitudinal salt transport in an idealized, partially mixed estuary. J. Phys. Oceanogr. 39, 1905–1920.
Codiga, D., Stoffel, H., Deacutis, C., Kiernan, S., Oviatt, C., 2009. Narragansett Bay hypoxic event characteristics based on fixed-site monitoring network time series: intermittency, geographic distribution, spatial synchrony, and interannual variability. Estuaries Coasts 32, 621–641.
Csanady, G., 1973. Wind-induced barotropic motions in long lakes. J. Phys. Oceanogr. 3 (4), 429–438.
Deacutis, C., Murray, D., Prell, W., Saarman, E., Korhun, L., 2006. Hypoxia in the upper half of Narragansett Bay, RI, during August 2001 and 2002. Northeast. Nat. 13 (Special Issue 4), 173–198.
Deacutis, C., 2008. Evidence of ecological impacts from excess nutrients in upper Narragansett Bay. In: Desbonnet, A., Costa-Pierce, B. (Eds.), Science for Ecosystem-Based Management: Narragansett Bay in the 21st Century. Springer, New York NY, pp. 349–381.
DeLeo, W., 2001. Investigation of the Physical Mechanisms Controlling Exchange Between Mount Hope Bay and the Sakonnet River (M.S. thesis). University of Rhode Island, Kingston RI.
Diaz, R., 2001. Overview of hypoxia around the world. J. Environ. Qual. 30, 275–281.
Dyer, K., 1997. Estuaries: A Physical Introduction, 2nd edition. Wiley, Chichester UK.
Ekman, V., 1905. On the influence of the Earth's rotation on ocean currents. Ark. Mat.Astrono. Fys. 2, 1–53.
Emery, W., Thomson, R., 2001. Data Analysis Methods in Physical Oceanography, 2nd edition. Elsevier, Amsterdam, The Netherlands.
Fewings, M., Lentz, S., Fredericks, J., 2008. Observations of cross-shelf flow driven by cross-shelf winds on the inner continental shelf. J. Phys. Oceanogr. 38, 2358–2378.
Furnas, M., Hitchcock, G., Smayda, T., 1976. Nutrient-phytoplankton relationships in Narragansett Bay during the 1974 summer bloom. In: Wiley, M. (Ed.), Estuarine Processes: Uses, Stresses and Adaptation to the Estuary, Volume 1. Academic Press, New York NY, pp. 118–134.
Garvine, R., 1985. A simple model of estuarine subtidal fluctuations forced by local and remote wind stress. J. Geophys. Res. 90 (C6), 11945–11948.
Geyer, W., 1997. Influence of wind on dynamics and flushing of shallow estuaries. Estuar. Coast. Shelf Sci. 44, 713–722.
Geyer, W.R., MacCready, P., 2014. The estuarine circulation. Annu. Rev. Fluid Mech. 46, 175–197.
Gill, A.E., 1982. Atmosphere-Ocean Dynamics. Academic Press.
Gill, A.E., Schumann, E.H., 1974. The generation of long shelf waves by the wind. J. Phys. Oceanogr. 4, 83–90.
Goodrich, D., 1988. On meteorologically induced flushing in three US east coast estuaries. Estuar. Coast. Shelf Sci. 26 (2), 111–121.
Gordon, R., Spaulding, M., 1987. Numerical simulation of the tidal and wind driven circulation in Narragansett Bay. Estuar. Coast. Shelf Sci. 24, 611–636.
GSO Fish Trawl, 2014. Graduate School of Oceanography Fish Trawl Survey. University of Rhode Island. Retrieved from ⟨http://www.gso.uri.edu/fishtrawl/⟩ (01.09.14.).
Guo, X., Valle-Levinson, A., 2008. Wind effects on the lateral structure of density-driven circulation in Chesapeake Bay. Cont. Shelf. Res. 28, 2450–2471.
Hansen, D.V., Rattray, M., 1965. Gravitational circulation in straits and estuaries. J. Mar. Res. 23, 104–122.
Hare, J., Govoni, J., 2005. Comparison of average larval fish vertical distributions among species exhibiting different transport pathways on the southeast United States continental shelf. Fish. Bull. 103, 728–736.
Hicks, S.D., 1959. The physical oceanography of Narragansett Bay. Limnolo. Oceanogr. 4, 316–327.
Huijts, K., Schuttelaars, H., de Swart, H., Friedrichs, C., 2009. Analytical study of the transverse distribution of along-channel and transverse residual flows in tidal estuaries. Cont. Shelf Res. 29, 89–100.
Janzen, C., Churchill, J., Pettigrew, N., 2005. Observations of exchange between eastern Casco Bay and the western Gulf of Maine. Deep-Sea Res. Part II 52, 2411–2429.
Janzen, C., Wong, K., 2002. Wind-forced dynamics at the estuary-shelf interface of a large coastal plain estuary. J. Geophys. Res. 107 (C10), 3138.
Jay, D.A., Smith, J.D., 1990. Circulation, density distribution and neap-spring transitions in the Columbia River Estuary. Prog. Oceanogr. 25, 81–112.
Jia, P., Li, M., 2012. Dynamics of wind-driven circulation in a shallow lagoon with strong horizontal density gradient. J. Geophys. Res. 117, C05013.
Jickells, T., 1998. Nutrient biogeochemistry of the coastal zone. Science 281, 217–222.
Kemp, W., Testa, J., Conley, D., Gilbert, D., Hagy, J., 2009. Temporal responses of coastal hypoxia to nutrient loading and physical controls. Biogeosciences 6, 2985–3008.
Kincaid, C., Bergondo, D., Rosenberger, K., 2008. The dynamics of water exchange between Narragansett Bay and Rhode Island Sound. In: Desbonnet, A., Costa-Pierce, B. (Eds.), Science for Ecosystem-Based Management: Narragansett Bay in the 21st Century. Springer, New York, NY, pp. 301–324.
Kincaid, C., Pockalny, R., Huzzey, L., 2003. Spatial and temporal variability in flow at the mouth of Narragansett Bay. J. Geophys. Res. 108 (C7), 1612–1626.
Kirincich, A., Barth, J., Grantham, B., Menge, B., Lubchenco, J., 2005. Wind-driven inner-shelf circulation off central Oregon during summer. J. Geophys. Res. 110, C10S03.
Klinck, J., O'Brien, J., Svendsen, H., 1982. A simple model of fjord and coastal circulation interaction. J. Phys. Oceanogr. 11, 1612–1626.
Knudsen, M., 1900. Ein hydrographischer Lehrsatz. Ann. Hydrogr. Marit. Meteorol. 28, 316–320.
Lentz, S.J., 1995. Sensitivity of the inner-shelf circulation to the form of the eddy viscosity profile. J. Phys. Oceanogr. 25, 19–28.
Lentz, S., 2001. The influence of stratification on the wind-driven cross-shelf circulation over the North Carolina shelf. J. Phys. Oceanogr. 31, 2749–2760.
Lentz, S.J., Fewings, M.R., 2012. The wind-and wave-driven inner-shelf circulation. Annu. Rev. Mar. Sci. 4, 317–343.
Lentz, S., Guza, R.T., Elgar, S., Feddersen, F., Herbers, T.H.C., 1999. Momentum balances on the North Carolina inner shelf. J. Geophys. Res. 104, 18205–18226.
Lerczak, J., Geyer, W., 2004. Modeling the lateral circulation in straight, stratified estuaries. J. Phys. Oceanogr. 34 (6), 1410–1428.
Li, Z., Weisberg, R.H., 1999a. West Florida shelf response to upwelling favorable wind forcing: kinematics. J. Geophys. Res. 104 (C6), 13507–13527.
Li, Z., Weisberg, R.H., 1999b. West Florida continental shelf response to upwelling favorable wind forcing: 2. Dynamics. J. Geophys. Res. 104 (C10), 23427–23442.
Li, Y., Li, M., 2011. Effects of winds on stratification and circulation in a partially mixed estuary. J. Geophys. Res. 116, C12012.
Li, Y., Li, M., 2012. Wind-driven lateral circulation in a stratified estuary and its effects on the along-channel flow. J. Geophys. Res. 117, C09005.
MacCready, P., Geyer, W., 2010. Advances in estuarine physics. Annu. Rev. Mar. Sci. 2, 35–58.
Monismith, S., 1986. An experimental study of the upwelling response of stratified reservoirs to surface shear stress. J. Fluid Mech. 171, 407–439.
Monsen, N., Cloern, J., Lucas, L., Monismith, S., 2002. A comment on the use of flushing time, residence time, and age as transport time scales. Limnol. Oceanogr. 47 (5), 1545–1553.
Narragansett Bay Window Program, 2014. Narragansett Laboratory, National Marine Fisheries Service. Retrieved from ⟨http://www.nefsc.noaa.gov/omes/OMES/nabay.html⟩ (01.09.14.).
Narvaez, D., Valle-Levinson, A., 2008. Transverse structure of wind-driven Flow at the entrance to an estuary: Nansemond River. J. Geophys. Res. 113, C09004.
NDBC BUZM3, 2011.NOAA National Data Buoy Center, Station BUZM3, Buzzards Bay, MA. Retrieved from ⟨http://www.ndbc.noaa.gov/station_page.php?station=buzm3⟩ (20.06.11.).
Nixon, S., Granger, S., Nowicki, B., 1995. An assessment of the annual mass balance of carbon, nitrogen, and phosphorus in Narragansett Bay. Biogeochemistry 31 (1), 15–61.
Nixon, S., Ammerman, J., Atkinson, L., Berounsky, V., Billen, G., Boicourt, W., Boynton, W., Church, T., Ditoro, D., Elmgren, R., Garber, J., Giblin, A., Jahnke, R., Owens, N., Pilson, M., Seitzinger, S., 1996. The fate of nitrogen and phosphorus at the land-sea margin of the North Atlantic Ocean. Biogeochemistry 35 (1), 141–180.
NOAA PORTS, 2011. NOAA Tides & Currents, Station 8452660, Newport, RI. Retrieved from ⟨http://tidesandcurrents.noaa.gov/ports/ports.html?id=8452660⟩ (20.06.11.).

Pawlowicz, R., 2001. A tracer method for determining transport in two-layer systems, applied to the Strait of Georgia/Haro Strait/Juan de Fuca Strait estuarine system. Estuar. Coast. Shelf Sci. 52, 491–503.
Pape, E., Garvine, R., 1982. The subtidal circulation in Delaware Bay and adjacent shelf waters. J. Geophys. Res. 87, 7955–7970.
Pilson, M., 1985. On the residence time of water in Narragansett Bay. Estuaries 8, 2–14.
Pilson, M.E.Q., 2008. Narragansett Bay amidst a globally changing climate. In: Desbonnet, A., Costa-Pierce, B. (Eds.), Science for Ecosystem-Based Management: Narragansett Bay in the 21st Century. Springer, New York NY, pp. 35–46.
Pritchard, D., 1956. The dynamic structure of a coastal plain estuary. J. Mar. Res. 15, 33–42.
Rogers, J., 2008. Circulation and Transport in Upper Narragansett Bay (Master's thesis). University of Rhode Island, Kingston RI.
Rosenberger, K., 2001. Vertical Structure of Tidal and Residual Currents in Rhode Island Sound (Master's thesis). University of Rhode Island, Kingston RI.
Saarman, E., Prell, W., Murray, D., Deacutis, C., 2008. Summer bottom water dissolved oxygen in upper Narragansett Bay. In: Desbonnet, A., Costa-Pierce, B. (Eds.), Science for Ecosystem-Based Management: Narragansett Bay in the 21st Century. Springer, New York NY, pp. 325–348.
Scully, M., Geyer, W., Lerczak, J., 2009. The influence of lateral advection on the residual estuarine circulation: a numerical modeling study of the Hudson River estuary. J. Phys. Oceanogr. 39 (1), 107–124.
Shonting, D., 1969. Rhode Island Sound square kilometer study 1967: flow patterns and kinetic energy distribution. J. Geophys. Res. 74, 3386–3395.
Shonting, D., Cook, G., 1970. On the seasonal distribution of temperature and salinity in Rhode Island Sound. Limnol. Oceanogr. 15, 100–112.
Simpson, J.H., Brown, J., Matthews, J., Allen, G., 1990. Tidal straining, density currents, and stirring in the control of estuarine stratification. Estuaries 13, 125–132.
Tilburg, C., Reager, J., Whitney, M., 2005. The physics of blue crab larval recruitment in Delaware Bay: a model study. J. Mar. Res. 3, 471–495.
USGS Blackstone, 2011. USGS National Water Information System, Site 01112500 Blackstone River at Woonsocket, RI. Retrieved from ⟨http://waterdata.usgs.gov/nwis/dv/?site_no=01112500⟩ (20.06.11.).
Valle-Levinson, A., Li, C., Royer, T., Atkinson, L., 1998. Flow patterns at the Chesapeake Bay entrance. Cont. Shelf Res. 18, 1157–1177.
Valle-Levinson, A., Lwiza, K., 1995. The effects of channels and shoals on exchange between the Chesapeake Bay and the adjacent ocean. J. Geophys. Res. 100 (C9), 18551–18563.
Wang, D.P., 1979. Wind-driven circulation in the Chesapeake Bay, winter 1975. J. Phys. Oceanogr. 9, 564–572.
Wang, D.P., Elliott, A.J., 1978. Non-tidal variability in the Chesapeake Bay and Potomac River: evidence for non-local forcing. J. Phys. Oceanogr. 8, 225–232.
Weisberg, R., 1976. The non-tidal flow in the Providence River of Narragansett Bay: a stochastic approach to estuarine circulation. J. Phys. Oceanogr. 6, 345–354.
Weisberg, R., Sturges, W., 1976. Velocity observations in the West Passage of Narragansett Bay: a partially mixed estuary. J. Phys. Oceanogr. 6, 345–354.
Weisberg, R.H., Black, B.D., Li, Z., 2000. An upwelling case study on Florida's west coa. J. Geophys. Res. 105 (C5), 11459–11469.
Weisberg, R.H., Li, Z., Muller-Karger, F., 2001. West Florida shelf response to local wind forcing. J. Geophys. Res. 106, 31239–31262.
Weisberg, R.H., He, R., Liu, Y., and Virmani, J.I. (2005). West Florida shelf circulation on synoptic, seasonal, and interannual time scales. In: Sturges, W. and Lugo-Fernandez, A. (Eds.) Circulation in the Gulf of Mexico: Observations and Models. (Geophysical Monograph Series), 161 American Geophysical Union, Washington DC 325–347.
Weisberg, R.H., Zheng, L., 2006. Circulation of Tampa Bay driven by buoyancy, tides, and winds, as simulated using a finite volume coastal ocean model. J. Geophys. Res. 111, C01005.
Whitney, M.M., Codiga, D.L., Ullman, D.S., McManus, P.M., Jiorle, R., 2012. Tidal cycles in stratification and shear and their relationship to gradient Richardson number and eddy viscosity variations in estuaries. J. Phys. Oceanogr. 42, 1124–1133.
Winant, C.D., 2004. Three-dimensional wind-driven flow in an elongated, rotating basin. J. Phys. Oceanogr. 34, 62–476.
Wong, K., 1994. On the nature of transverse variability in a coastal plain estuary. J. Geophys. Res. 99, 14.
Wong, K., Munchow, A., 1995. Buoyancy forced interaction between estuary and inner shelf: observation. Cont. Shelf Res. 15 (1), 59–88.
Wong, K., Valle-Levinson, A., 2002. On the relative importance of the remote and local wind effects on the subtidal exchange at the entrance to the Chesapeake Bay. J. Mar. Res. 60, 477–498.